

## Original Article

# Increased FOXA1 levels induce apoptosis and inhibit proliferation in FOXA1-low expressing basal breast cancer cells

Ke Xia, Wenqiang Huang, Xiaoyun Zhao, Xiaoqin Huang, Yan Chen, Li Yu, Yongjun Tan

State Key Laboratory of Chemo/Biosensing and Chemometrics, College of Biology, Hunan Engineering Research Center for Anticancer Targeted Protein Pharmaceuticals, Hunan University, Changsha 410082, Hunan, China

Received January 12, 2022; Accepted May 25, 2022; Epub June 15, 2022; Published June 30, 2022

**Abstract:** The transcription factor FOXA1, which is a member of the forkhead class of DNA-binding proteins, interacts with Estrogen Receptor (ER) to mediate breast cancer progression. However, its role in basal breast cancer cells remains unclear. Although the overall levels of FOXA1 are decreased in the basal subtype of clinical TCGA breast cancer samples, the high levels of FOXA1 improve the survival of the patients from this subtype. This clinical phenomenon is consistent with that of FOXA1 stimulating apoptosis in FOXA1-low expressing basal breast cancer cells, such as MDA-MB-231, and MDA-MB-468 cells. In this study, we have constructed an inducible expression system of FOXA1 and demonstrated the induced expression of FOXA1 resulting in apoptosis and cell cycle arrest in MDA-MB-231 cells, as confirmed by transcriptomic analysis and *in vivo* tumor-grafted models. Furthermore, the low levels of Estrogen Receptor-1 (ESR1) are critical for FOXA1 in terms of its repressive roles in the cells, as evidenced by clinical data analysis indicating that the high levels of FOXA1 improve the survival of ESR1<sup>Low</sup> patients, but worsen the survival of ESR1<sup>High</sup> patients of breast cancer. When introduced into MDA-MB-231 cells, ESR1 counteracts the tumor suppressor roles of FOXA1 by altering the FOXA1-regulated gene transcription and the two proteins together maintain the tumor progression *in vivo*. Our cumulative results suggest that FOXA1 suppresses the basal breast cancer cells with FOXA1-low expressing status independent of ESR1 by inducing apoptosis and inhibiting cell proliferation, thereby implicating its potential therapeutic role in this group of breast cancer.

**Keywords:** Transcription factor FOXA1, estrogen receptor-1 (ESR1), apoptosis, cell proliferation, basal breast cancer

## Introduction

Breast cancer is the leading serious cancer affecting women across the world and represents a complex and heterogeneous disease comprising diverse pathologies, histological features, and clinical implications [8]. The molecular classification of breast cancer has identified 5 distinct subtypes: normal breast-like, luminal A, luminal B, human epithelial growth factor receptor-2 (Her-2) overexpressing, and basal breast cancer [38]. Among these, basal breast cancer is characterized by the lack of Estrogen Receptor (ER), Progesterone Receptor (PR), or Her-2 expression, albeit expressing basal cytokeratins and epidermal growth factor receptor [49] and associated with an aggressive phenotype, high histological

grade, poor clinical behavior, and high rates of recurrences and/or metastasis [25]. The lack of ER/PR and Her-2 renders basal breast cancer especially refractory to hormone therapy or Her-2-targeted therapy. As a result, there are only a few therapeutic options presently for basal breast cancer with a poor overall prognosis of this subtype, leading to a relatively high mortality rate [1]. Therefore, it is of utmost priority to study the molecular mechanisms regulating this subtype specifically in order to develop new potential therapeutic strategies for the treatment of basal breast cancer.

Transcription factor FOXA1 (previously known as HNF-3 $\alpha$ ), which was originally identified for its transcriptional regulation of liver-specific genes [17], is the founding member of the FOX

## FOXA1 represses basal breast cancer cells

transcription factor family comprising at least 40 members [28]. FOXA1 plays important roles during embryonic development [24] and exhibits emerging roles in cancers [34]. The expression of FOXA1 during gastrulation signifies its regulatory functions during the early development of embryos [2]. The FOXA1 expression ranges in adults includes tissues derived from the endoderm (e.g., prostate, liver, lung, pancreas, stomach, intestine, and bladder), mesoderm (e.g., mammary glands, kidney, vagina and uterus, and seminal and coagulating glands), and neurectoderm (e.g., brain and olfactory epithelium) [5], indicating its multiple functions in different adult organs. It also participates in stimulating the differentiation of pluripotent stem cells [47]. Over the past decade, FOXA1 has been examined in several human cancers and proposed to exhibit oncogenic and tumor-suppressive roles, depending on the cancer type or subtype [4]. For example, the FOXA1 levels increase in the cancers of lung, esophageal, and thyroid, implicating its role in promoting tumorigenesis or tumor progression in these tissues [29, 36]. In contrast, elevated FOXA1 levels have been reported to inhibit the cell proliferation of prostate cancer [50] and hepatocellular carcinoma (HCC) [18]. In addition, FOXA1 prevents the epithelial to mesenchymal transition of pancreatic cancer cells [45], implying its suppressive role in the cancer. In certain circumstances, such as in metformin-treated HCC HepG2 cells or under the oxidative stress of lung cancer A549 cells, the FOXA1 expression is induced to consequently result in cell apoptosis [44, 46], which further supports its suppressive roles in certain cancers.

FOXA1 has also been heavily investigated in breast cancer, with potential variant roles depending on the ER status and tumor molecular subtypes. In normal breast tissues, FOXA1 and ER show a strong co-expression in luminal breast cancer, and similar to those of ER, high FOXA1 levels are associated with low tumor grade and good cancer prognosis [48]. Accordingly, low FOXA1 levels correlate with the diagnostic markers of poor prognosis, including the basal subtype, high-grade, increased tumor size, and nodal metastasis [33]. Functioning as a transcription factor, FOXA1 cooperates with Estrogen Receptor-1 (ESR1) [26] in regulating the gene expression in ER-positive luminal breast cancer cells, as evidenced by FOXA1

occupying over half of the ESR1-binding sites in the genome [9]. Consequently, FOXA1 is deemed essential for the cellular response to the ER antagonist tamoxifen [27], which is a therapeutic option for luminal breast cancer through the induction of ESR1 association with estrogen-stimulated gene loci while suppressing the gene expression [42]. FOXA1 is necessary for ESR1-mediated cell-cycle progression through the FOXA1-associated ESR1 stimulation of cyclin D1 [19], which suggests that FOXA1 promotes the progression of luminal breast cancer through ESR1-dependent mechanisms. Although FOXA1 statistically correlates with ESR1 in clinical breast cancer samples, some cases of ER-negative breast cancer have been reported to possess high FOXA1 expression [23], implicating ESR1-independent functions of FOXA1 in breast cancer. In this study, we noticed that the high levels of FOXA1 could improve the survival of the patients not only from the subtype of basal breast cancers but also from the group of ESR1<sup>Low</sup> breast cancers. Consistent with this observation, it has been reported that FOXA1 prevents the epithelial to mesenchymal transition and cell proliferation of basal breast cancer cells through the activation of the transcription of E-cadherin [30] and p27Kip1 [51] independent of ESR1, further indicating the suppressive role of FOXA1 in this subtype of breast cancers.

In this study, we intended to confirm the repressive effects of FOXA1 on basal breast cancer with FOXA1-low expressing status and explore the mechanisms underlying how FOXA1 suppresses the cells. We observed that the elevation of the FOXA1 levels induced apoptosis and inhibited the proliferation in FOXA1-low expressing basal breast cancer cells but not in FOXA1-high expressing basal or non-basal breast cancer cells. Moreover, we found that the low levels of ESR1 were required for FOXA1 to perform its repressive roles. ESR1 counteracted the roles of FOXA1 as a tumor suppressor by altering the FOXA1 alone-regulated gene transcription, and the two proteins together maintained the tumor progression of the cells. Cumulatively, our results demonstrated that FOXA1 could suppress the FOXA1-low expressing basal breast cancer independent of ESR1 and promoting the expression of FOXA1 could be a potential application in developing a therapeutic strategy for the treatment of this group of breast cancers.

# FOXA1 represses basal breast cancer cells

## Materials and methods

### *Clinical data and bioinformatic analysis*

Clinical breast cancer samples (n=1122) were collected from The Cancer Genome Atlas (TCGA) database. The analysis of FOXA1 levels in the subgroups of breast cancer and the correlation between FOXA1 and ESR1 were executed by using ggstatsplot package through R project (<http://www.r-project.org>). For survival curve analysis, the basal subgroup (n=220) and the non-basal subgroup (n=827) were extracted from the data set and two ESR1-related data sets, in which the ESR1<sup>High</sup> subgroup (n=349) or the ESR1<sup>Low</sup> subgroup (n=349) contained either the top 1/3 or the bottom 1/3 of total cancer samples (n=1047) respectively according to the levels of ESR1, were also extracted. FOXA1-related survival of patients was fitted by the 'survfit' function, and Kaplan-Meier curves were drawn by the 'ggsurv' function in the R package 'survival'. The cut-off value of FOXA1 high or low expression was determined by setting 'minprop' parameter to 0.1.

The RNA sequencing was performed by HUADA Gene Company of China and the bioinformatic analysis of the data was executed by using GEOquery, ggplot2, and clusterProfiler packages through R project (<http://www.r-project.org>).

### *Cell culture*

Human cell lines MCF-7, MDA-MB-231, MDA-MB-468, MDA-MB-453, and HEK293T were purchased from the Cell Bank of Chinese Academy of Sciences. MCF-7, MDA-MB-231, and HEK293T cells were maintained in DMEM containing 10% fetal bovine serum. MDA-MB-468 and MDA-MB-453 cells were maintained in L-15 medium containing 10% fetal bovine serum. Based on MDA-MB-231 cells, the home-made 231-FOXA1-ind and ESR1-231-FOXA1-ind cell lines and corresponding control cell lines (231-Con-ind and Con-231-FOXA1-ind) were generated by the infection of certain lentiviruses followed by puromycin selection. The primers specific to the puromycin resistant gene in pLVX-TetOne-Puro vector (Clontech), sense (S): 5'-CGA CCA TGA CCG AGT ACA AG-3' and antisense (AS): 5'-GGG CGC GGA GGT CTC CAG GA-3', were used for PCR to confirm the correct single-cell clones with the extracted genomic DNA of the cells.

### *Plasmid construction and transfection*

The cDNAs of human FOXA1 (Gene ID: 3169) and ESR1 (Gene ID: 2099) were purchased from Changsha Yingrun Biotechnology of China. FOXA1 cDNA was PCR amplified with primers containing BamHI and XbaI sites (S: 5'-GCG GAT CCA TGT TAG GAA CTG TGA AGA TGG AA-3' and AS: 5'-GCT CTA GAC TAG GAA GTG TTT AGG ACG GGT CT-3') and ligated into a lentivirus plasmid vector (Shanghai SiDanSai Biotech, China) to obtain pLv-FOXA1, or ligated into pcDNA3.1 vector (Invitrogen) to obtain pCMV-FOXA1. To generate pHis-FOXA1, primers containing BamHI and XbaI sites (S: 5'-GCG GAT CCA TGC ATC ACC ATC ACC ATC ACT TAG GAA CTG TGA AGA TGG AA-3' and AS: 5'-GCT CTA GAC TAG GAA GTG TTT AGG ACG GGT CT-3') were used to amplify FOXA1 cDNA to ligate into pcDNA3.1 vector. To generate pLv-TetOne-FOXA1, primers containing EcoRI and BamHI sites (S: 5'-GCG AAT TCA TGT TAG GAA CTG TGA AGA T-3' and AS: 5'-GCG GAT CCC TAG GAA GTG TTT AGG ACG G-3') were used to amplify FOXA1 cDNA to ligate into pLVX-TetOne-Puro vector (Clontech). To generate pLv-ESR1, primers containing BamHI and Ascl sites (S: 5'-GCG GAT CCA TGA CCA TGA CCC TCC ACA C-3' and AS: 5'-CGG GCG CGCCT CAG ACC GTG GCA GGG AAA CCC T-3') were used to amplify ESR1 cDNA to ligate into the lentivirus plasmid vector. To generate pCMV-ESR1, primers containing BamHI and XhoI sites (S: 5'-GCG GAT CCA TGA CCA TGA CCC TCC ACA C-3' and AS: 5'-GCC TCG AGT CAG ACC GTG GCA GGG AAA CCC T-3') were used to amplify ESR1 cDNA to ligate into pcDNA3.1 vector. To generate pFlag-ESR1, primers containing BamHI and XhoI sites (S: 5'-GCG GAT CCA TGA CCA TGA CCC TCC ACA C-3' and AS: 5'-CGC TCG AGT CAC TTA TCG TCG TCA TCC TTG TAA TCG ACC GTG GCA GGG AAA CCC T-3') were used to amplify ESR1 cDNA to ligate into pcDNA3.1 vector.

The human BIK upstream promoter regions (-1800 to +100 bp) were PCR amplified from 293T genomic DNA with the primers (S: 5'-GCT CTT TTC TGC TAA TGT TTA CTG A -3' and AS: 5'-GCT CGA GCT GGG CGG AGC AGC GGG C-3') and ligated into the pGL3-basic vector to obtain the plasmid pBIKpro (-1.8 kb)-Luc. The transfection of plasmids to certain cells was routinely performed with Lipofectamine 2000 (Invitrogen) according to the manufacturer's protocol.

## FOXA1 represses basal breast cancer cells

### *Lentivirus preparation and infection*

The pLv-Con, pLv-FOXA1, pLv-ESR1, pLv-TetOne-Con, or pLv-TetOne-FOXA1 plasmids were transfected into 293T cells with two packaging plasmids (pVSVG and  $\Delta 8.91$ ) by calcium phosphate. Forty-eight hours post transfection, the medium of 293T was collected and filtered with 0.22  $\mu\text{m}$  filter to obtain lentiviruses (Lv-Con, Lv-FOXA1, Lv-ESR1, Lv-TetOne-Con, or Lv-TetOne-FOXA1). The titration of the lentivirus was measured by flow cytometry (Beckman). Usually, the tested cells were infected with a lentivirus (20 pfu/cell). The infected cells were confirmed by flow cytometry according to the EGFP expression of the lentivirus. To obtain 231-FOXA1-ind and 231-Con-ind cells, MDA-MB-231 cells were infected with Lv-TetOne-FOXA1 or Lv-TetOne-Con (20 pfu/cell, 48 hrs) and treated with puromycin (2 mg/mL, 72 hrs) for cell line selection. The single-cell clones were sorted by flow cytometry according to the EGFP expression. To obtain ESR1-231-FOXA1-ind and Con-231-FOXA1-ind cells, 231-FOXA1-ind cells were infected with Lv-ESR1 or Lv-Con (20 pfu/cell). To obtain ESR1-231-Con-ind and Con-231-Con-ind cells, 231-Con-ind cells were infected with Lv-ESR1 or Lv-Con (20 pfu/cell).

### *Quantitative real-time PCR (qPCR)*

Total RNA was extracted with Trizol reagent (Omega) according to the manufacturer's instructions. Total RNA (2  $\mu\text{g}$ ) was reverse transcribed into 20  $\mu\text{l}$  cDNA by RevertAid First Strand Kit (Promega). The qPCR was performed with SYBR Green (Toyobo) with following primers: hFOXA1-S, 5'-GCA ATA CTC GCC TTA CGG CT-3' and hFOXA1-AS, 5'-TAC ACA CCT TGG TAG TAC GCC-3'; hESR1-S, 5'-AAA TTC AGA TAA TCG ACG CC-3' and hESR1-AS, 5'-TGC ACA CTG CAC AGT AGC GA-3'; hPCNA-S, 5'-CCT GCT GGG ATA TTA GCT CCA-3' and hPCNA-AS, 5'-CAG CGG TAG GTG TCG AAG C-3'; hCDC25C-S, 5'-CCC TGA AAG ATC AAG AAG CA-3' and hCDC25C-AS, 5'-GTC CTT GAA TTT TTC CAC CT-3'; hMCM8-S, 5'-ATA CAG TCT TCC CAC AAA GT-3' and hMCM8-AS, 5'-ATC AAT TCC TGG ATT TTG AT-3'; hBIK-S, 5'-GAC GAG ATG GAC GTG AGC CT-3' and hBIK-AS, 5'-TCT AAG AAC ATC CCT GAT GT-3'; and hGAPDH-S, 5'-GGA GCG AGA TCC CTC CAA AAT-3' and hGAPDH-AS, 5'-GGC TGT TGT CAT ACT TCT CAT GG-3'. The qPCR was performed in the realplex2 qPCR system (Eppendorf). Relative

mRNA levels were normalized to the levels of GAPDH.

### *Protein extraction and western blotting*

To obtain protein extracts, cells were washed with chilled PBS and scraped from culture dishes in lysis buffer (0.5% NP-40, 50 mM Tris-HCl PH 7.5, 100 mM NaCl, 0.1 mM  $\text{Na}_3\text{VO}_4$ , 1 mM NaF, 2.5 mM EDTA, 2.5 mM EGTA, 5% Glycerin, 10 mM  $\beta$ -glycerophosphate, protease inhibitor mixture). Tumor tissue were homogenized using the TissueLyser (Qiagen) and lysed in buffer containing 50 mM Tris-HCl PH 8.0, 150 mM NaCl, 2 mM EDTA PH 8.0, 10 mM NaF, 20% glycerol, 1% Nonidet P-40 plus protease inhibitors. The protein concentration was measured using the BCA protein assay reagent (Thermo Fisher Scientific). To prepare cytoplasmic and nuclear extract, cell pellets were suspended in CE buffer (10 mM HEPES PH7.9, 1.5 mM  $\text{MgCl}_2$ , 10 mM KCl, containing protease inhibitor) and incubated on ice for 5 min. An equal amount of CE buffer containing 0.2% NP40 was added to the cell suspension, incubated for 5 min on ice, and centrifuged for 3 min at 6500 rpm at 4°C. The supernatant was the cytoplasmic extract. The pellet was resuspended in NE buffer (20 mM HEPES PH7.9, 1.5 mM  $\text{MgCl}_2$ , 0.42 M NaCl, 0.2 mM EDTA, 25% glycerol, containing protease inhibitors) and vortexed at full speed for 1 min. The nuclear extract suspension underwent three cycles of freeze (-80°C, 15 min) and thaw (37°C, 1 min). Between each cycle of freeze/thaw the suspension was vortexed for 1 min at full speed. The suspension was then spun at full speed for 15 min at 4°C. The supernatant was the nuclear extract.

Lysates were mixed with beta-mercaptoethanol-containing sample buffer, heated to 95°C for 10 min. The lysates were separated using SDS-PAGE and transferred onto PVDF membrane for western blotting. The following antibodies and dilutions were used for Western blotting: rabbit anti-FOXA1 (1:3000, Abcam ab23738, UK), rabbit anti-Casp3 (active) (1:1000, Sangon D260009, China), mouse anti-PCNA (1:10000, Abcam ab29, UK), rabbit anti-BIK (1:1000, Abcam ab52182, UK), rabbit anti-CDC25C (1:1000, Sangon D155201, China), rabbit anti-MCM8 (1:1000, Sangon D220967, China), rabbit anti-ESR1 (1:1000, Beyotime AE905, China), mouse anti-Lamin

## FOXA1 represses basal breast cancer cells

A/C (1:1000, SantaCruz sc-7293, USA), mouse anti- $\alpha$ -Tubulin (1:1000, SantaCruz sc-53646, USA), and mouse anti- $\beta$ -actin (1:10000, Abcam ab49900, UK). Signals from the primary antibody were amplified by horseradish peroxidase (HRP) conjugated anti-rabbit IgG (1:5000, Beyotime A0303, China) or anti-mouse IgG (1:10000; BioRad 170-6516, USA), and detected with Super Signal West Femto Maximum Sensitivity Substrate (Thermo Fisher Scientific) by Kodak 4000 MM Imaging System (Kodak). The bands of Western blotting were quantified by ImageJ software.

### *Apoptosis analysis*

The tested cells were harvested by trypsinization and fixed with 4°C 70% ethanol. Intracellular DNA was stained with 50  $\mu$ g/ml propidium iodide in the dark for 30 min at room temperature and the samples were filtered and analyzed for the percentage of apoptotic bodies on Quanta SC flow cytometer (Beckman). Apoptotic DNA fragmentation was examined using the One-Step TUNEL Apoptosis Assay kit (C1089, Beyotime, China) according to the manufacturer's protocol. Briefly, cells were fixed in 4% paraformaldehyde for 30 min at 4°C and permeabilized in 0.1% Triton X-100 for 2 min on ice. After the TUNEL assay, the fluorescent signals were imaged with a FluoView FV1000 confocal imaging system (Olympus) by laser at 550 nm.

### *Proliferation analysis*

EDU staining was performed with BeyoClick™ EdU Cell Proliferation Kit (C0085S, Beyotime, China) following to the manufacturer's instructions. In brief, the tested cells were seeded in 6-well plates ( $1 \times 10^4$  cells/well) and two days later incubated with EDU for 2 hrs at 37°C. Then the cells were washed by PBS for three times and fixed with 4% paraformaldehyde. After incubating with 0.3% Triton X-100, the cells were stained with Click Addictive Solution A. The images were taken by TE2000 microscope (Nikon). To perform colony formation assays, the tested cells were seeded in 6-well plates ( $6 \times 10^2$  cells/well) and cultured at 37°C for 8 days. The cells were fixed with 4% paraformaldehyde and stained with 0.1% crystal violet for 15 min. The images were taken by TE2000 microscope.

### *Immunohistochemistry*

The collected tumor tissues were fixed with 4% paraformaldehyde and embedded in paraffin. For immunohistochemistry staining, the tumor sections (4  $\mu$ m) were dewaxed and rehydrated followed by endogenous peroxidase quenching, antigen retrieval (saline sodium citrate, microwaving), and non-specific binding site blocking. The sections were incubated subsequently with rabbit anti-Casp3 (active) (1:1000, Sangon D260009, China), rabbit anti-FOXA1 (1:3000, Abcam ab23738, UK), or rabbit anti-BIK (1:1000, Abcam ab52182, UK) followed by the incubation of a horseradish peroxidase conjugated anti-rabbit secondary antibody. Color was detected with 3, 3'-diaminobenzidine and pictures were taken at 200 $\times$  magnification by TE2000 microscope.

### *Chromatin immunoprecipitation (ChIP) assays*

ChIP assays were performed as previously described [53]. The following antibodies (2  $\mu$ g of each) were used for immunoprecipitation: rabbit anti-FOXA1 (Abcam ab23738), rabbit anti-IgG (Millipore PP64). The ChIP DNA samples were used in qPCR with the following primers: BIK upstream -1786 bp S, 5'-AGC ATA TTG TCT TGG GAT TTT G-3' and -1776 bp AS, 5'-ACC TGA TAT ATG TGA GAT GCT T-3'; BIK upstream -1206 bp S, 5'-GCC ACT GCA CTC CAG CCT GG-3' and -1196 bp AS, 5'-AAG TGT GAT AAA GTC TTC AGA-3'.

### *Electrophoretic mobility shift assays (EMSAs)*

The double-strand DNA (dsDNA) probe was synthesized by Sangon of China, based on the following sequence: dsDNA (BIK -1206 to -1196) probe: forward strand 5'-FAM-AAA ACA AAA ACA AAC AAA AAA-3' (Hot) or 5'-AAA ACA AAA ACA AAC AAA AAA-3' (Cold), and reverse strand 5'-TTT TTT GTT TGT TTT TGT TTT-3', dsDNA Mutation (BIK -1206 to -1196) probe: forward strand 5'-FAM-AAA ACG GGG GCG GGC TAA AAA-3' (Hot) and reverse strand 5'-TTT TTA GCC CGC CCC CGT TTT-3'. In the binding reactions, 10  $\mu$ g of nuclear proteins isolated from FOXA1-expressing cells, ESR1-expressing cells, or FOXA1 and ESR1 co-expressing cells was incubated with FAM-labeled probe (50 nM) in binding buffer (20 mM Tris-Cl, 50 mM KCl, 10% glycerol, 0.5 mM EDTA, 0.2 mM DTT, PH 7.6) for 30 min on ice. The reactions were resolved in 4%

## FOXA1 represses basal breast cancer cells

native polyacrylamide gel electrophoresis in 0.5×TBE and visualized with Kodak 4000 MM Imaging System (Kodak) (EX: 465 nm, EM: 535 nm for FAM).

### *Luciferase activity assays*

293T cells ( $1 \times 10^5$  cells/well in a 12-well plate) were transfected with pBIKpro (-1.8 kb)-Luc reporter plasmid (1  $\mu$ g) and certain expression vectors (1  $\mu$ g pCMV-FOXA1, plus 0.5  $\mu$ g or 1  $\mu$ g pCMV-ESR1). The pRL-CMV plasmid (20 ng) was used as the loading control for each transfection. The luciferase enzyme activities were measured 2 days later with the Dual-Luciferase Assay System (Promega, USA) following the manufacturer's instructions.

### *Animal experiments*

All animal experiments were performed in accordance with a protocol approved by the Ethics Review Committee, College of Biology, Hunan University, following institutional animal care and use guidelines by the Laboratory Animal Center of Hunan, China (Protocol No. SYXK [Xiang] 2018-0006). BALB/c nude mice (female, 4-week old) were purchased from Slac Experimental Animal Company (Changsha, China). The tested cells were implanted subcutaneously at left or right axilla of mice ( $5 \times 10^5$  cells/mouse) ( $n=6$  for each group). From Day 1 post injection, the mice were fed with water containing 1 mg/ml Doxycycline and the tumors were measured at every three days. At Day 27 post injection, the tumors were collected and the samples were prepared for immunohistochemistry, qPCR, or Western blotting.

### *Statistical analysis*

We used Microsoft Excel Program to calculate SD and statistically significant differences between samples and Used GraphPad Prism to draw the bar graph. The asterisks in each graph indicated statistically significant changes with *P*-values calculated by Student T Test: \* $P < 0.05$ , \*\* $P < 0.01$ , and \*\*\* $P < 0.001$ . *P*-values  $< 0.05$  were considered statistically significant.

## Results

### *FOXA1 stimulated apoptosis in FOXA1-low expressing basal breast cancer cells*

We first analyzed the FOXA1 expression levels in the clinical breast cancer samples ( $n=1122$ )

from the TCGA database and found that the average FOXA1 level in the basal subgroup (Basal,  $n=220$ ) was lower than that in the normal breast tissues (Normal,  $n=75$ ), while its average level in the other four breast cancer subgroups (Normal-like,  $n=89$ ; Luma,  $n=318$ ; LumB,  $n=275$ ; and Her-2,  $n=145$ ) was higher than that in the normal tissue group (**Figure 1A**). We noticed that the individual levels of FOXA1 in the patients of each subtype group varied dramatically and found that the patients with a high level of FOXA1 performed better in terms of survival compared to the patients with low levels of FOXA1 in the basal subgroup ( $n=220$ ) (**Figure 1B**). However, we found that the high levels of FOXA1 worsened the survival probability for the non-basal patients ( $n=827$ ) (**Figure 1B**), which implicates different roles of FOXA1 between basal and non-basal breast cancers. We also noticed the existence of different levels of FOXA1 among breast cancer cell lines, wherein basal breast cancer MDA-MB-231 and MDA-MB-468 cells exhibited extremely low levels of FOXA1 when compared to non-basal breast cancer MCF-7 and MDA-MB-453 cells (**Figure S1**). To test whether increasing FOXA1 levels could repress FOXA1-low expressing basal breast cancer cells, we constructed a FOXA1-expressing lentivirus to overexpress FOXA1 in these cells (**Figure S2**). The elevated levels of FOXA1 increased the levels of the activated caspase-3 [21] in FOXA1-low expressing MDA-MB-231 and MDA-MB-468 cells (**Figure 1C**), but not in FOXA1-high expressing MDA-MB-453 or MCF-7 cells (**Figure S3**). The apoptotic bodies in the cell samples were estimated by flow cytometry and the apoptosis ratio in MDA-MB-231 and MDA-MB-468 cells was also significantly increased by the FOXA1 overexpression (**Figure 1D**). Together, these results implicated that FOXA1 might repress certain basal breast cancer cells with FOXA1-low expressing status by stimulating apoptosis.

### *The induced expression of FOXA1 stimulated apoptosis and inhibited proliferation in basal breast cancer MDA-MB-231 cells*

To examine the repressive roles of FOXA1 to FOXA1-low expressing basal breast cancer cells in detail, we obtained single-cell clones from MDA-MB-231 cells infected by a lentivirus containing tetracyclin-induced cassette for the FOXA1 expression (**Figure S4**). The levels of FOXA1 could be induced by doxycycline treat-

## FOXA1 represses basal breast cancer cells

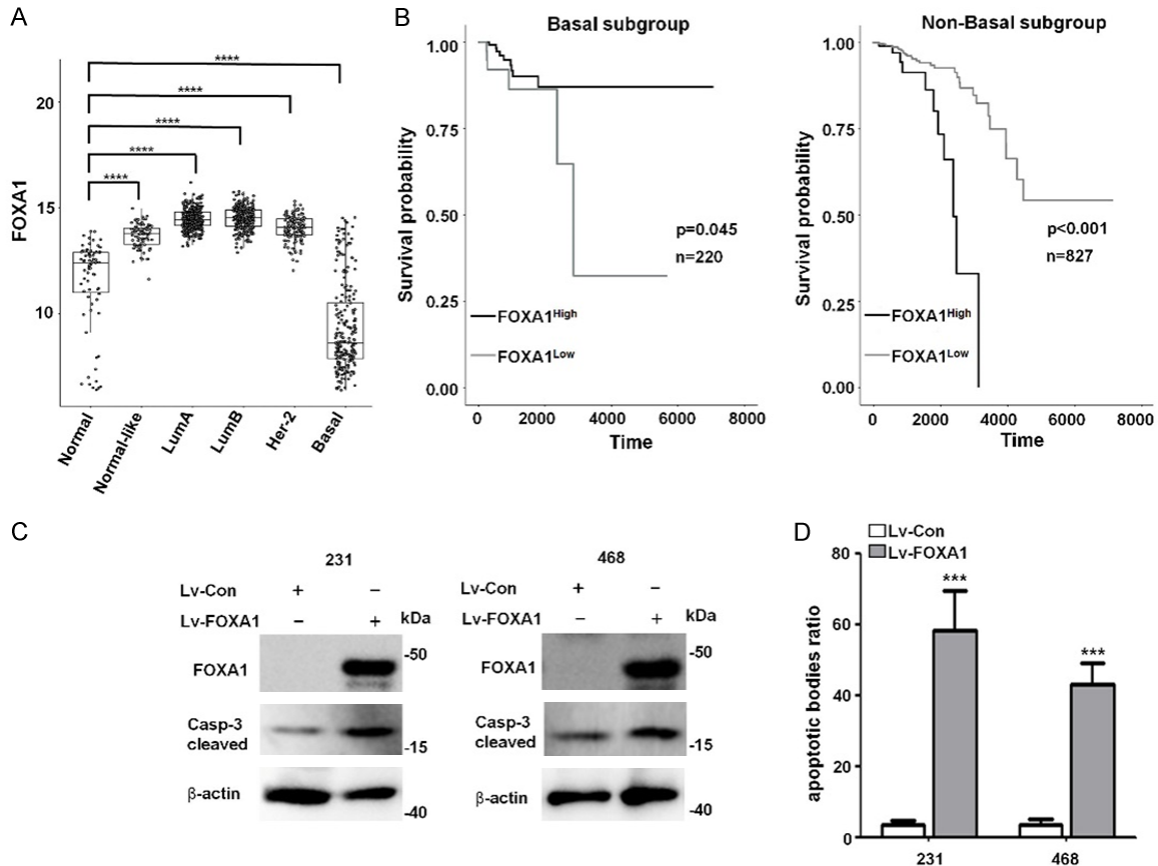


**Figure 1.** FOXA1 stimulated the apoptosis in basal breast cancer MDA-MB-231 and MDA-MB-468 cells. **A.** The levels of FOXA1 in normal breast tissue and the five subtypes (Normal, n=75; Normal-like, n=89; LumA, n=318; LumB, n=275; Her-2, n=145; and Basal, n=220) of breast cancer from the clinical breast cancer samples (the TCGA BRCA data set, n=1122). **B.** The high levels of FOXA1 improved the survival in basal breast cancer patients. FOXA1-related survival of patients in the basal BRCA data set (n=220) or the non-basal BRCA data set subgroup (n=827) was fitted by the 'survfit' function and Kaplan-Meier curves were drawn by the 'ggsurv' function in the R package 'survival'. The cut-off value of FOXA1 high or low expression was determined by setting 'minprop' parameter to 0.1. **C.** The overexpression of FOXA1 induced the levels of the activated Caspase-3 in FOXA1-low expressing basal breast cancer cells. Basal breast cancer MDA-MB-231 (231) and MDA-MB-468 (468) cells were infected by FOXA1-expressed lentivirus (Lv-FOXA1) or control lentivirus (Lv-Con) (20 pfu/cell) and protein lysates were prepared at Day 2 post infection. The levels of FOXA1 and activated caspase-3 (Casp-3 cleaved) in the cells were examined by Western blotting with FOXA1-specific antibody and cleaved caspase-3-specific antibody. The  $\beta$ -actin levels were measured as loading controls. **D.** The overexpression of FOXA1 elevated the levels of apoptotic bodies in basal breast cancer cells. 231 and 468 cells were infected with Lv-FOXA1 or Lv-Con, and the percentage of apoptotic bodies in samples were measured by PI-staining and Flow cytometry at Day 2 post infection. The measured values from Lv-Con-infected samples of each cell line were referred as 1. The asterisks indicate statistically significant changes: \*\*\* $P \leq 0.001$  and \*\*\*\* $P \leq 0.0001$ .

ment in the selected single-cell clones (n=6), whose cell numbers decreased after 2 days of induction of the FOXA1 expression when compared to that of parent MDA-MB-231 cells or the Lv-TetOne-Con-infected control cells (231-Con-ind cells) (Figure S5). We selected the cells of clone 2 for further investigations and confirmed that the decreased numbers of the cells and the induced levels of FOXA1 expression depended on the doxycycline dose (Figure

S6A, S6B). We found that treatment with 2  $\mu$ g/mL doxycycline could induce the expression of FOXA1 in MDA-MB-231 cells to similar levels as that of endogenous FOXA1 in MCF-7 cells (Figure S6C), causing an evident decrease in cell viability but not in 231-Con-ind cells (Figure S6D). The treatment of doxycycline alone demonstrated no toxic effects on MDA-MB-231 or 231-Con-ind cells even at concentration as high as 8  $\mu$ g/mL (Figure S7). We, therefore,

## FOXA1 represses basal breast cancer cells

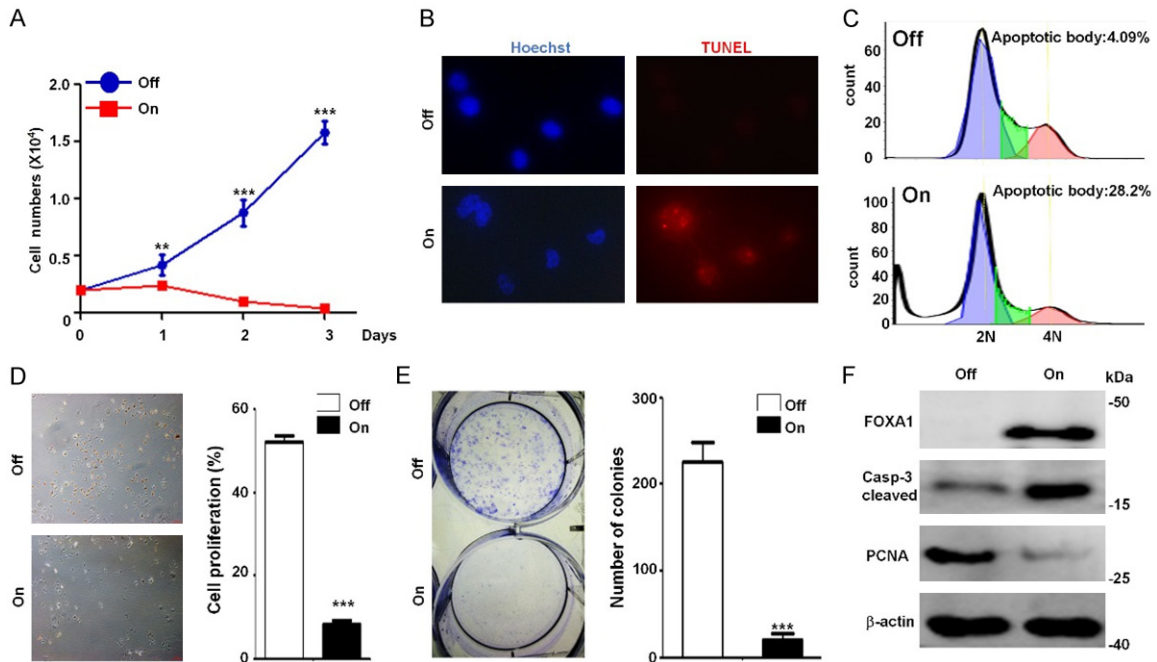


**Figure 2.** The induced expression of FOXA1 stimulated apoptosis and inhibited proliferation in basal breast cancer MDA-MB-231 cells. (A) The 231-FOXA1-ind cells ( $2 \times 10^3$  cells) were treated with doxycycline ( $2 \mu\text{g}/\text{mL}$ ) (On) or not (Off), and cell numbers were measured at Day 1, Day 2, and Day 3 post the treatment. (B, C) FOXA1 stimulated apoptosis in the cells. The 231-FOXA1-ind cells were treated as above. At Day 2 post the treatment, the TUNEL assays were performed with the One-Step TUNEL Apoptosis Assay Kit (Beyotime Biotechnology) and the typical TUNEL positive staining was detected in the FOXA1-On cells (B). The apoptotic bodies in the cell samples were measured by PI-staining and Flow cytometry (C). (D, E) FOXA1 inhibited proliferation in the cells. The 231-FOXA1-ind cells were treated as above and the proliferation of the cells were measured by the BeyoClick™ EdU Cell Proliferation Kit with DAB (Beyotime Biotechnology) at Day 2 post the treatment. The numbers of EdU-positive cells were counted from random selected fields ( $n=3$ ) to calculate the percentage of proliferative cells (D). The colony formation assays were also performed with the FOXA1-Off and FOXA1-On cells ( $6 \times 10^2$  cells/well). The cells were fixed at Day 14 post the treatment and the colonies were imaged by crystal violet staining. The numbers of colonies were counted and the graph represented the numbers  $\pm$  SD of colonies/well ( $n=3$ ) (E). (F) The protein lysates were prepared from the FOXA1-Off and FOXA1-On cells at Day 2 post the doxycycline ( $2 \mu\text{g}/\text{mL}$ ) treatment. The levels of FOXA1, activated caspase-3 (Casp-3 cleaved), and PCNA in the cells were examined by Western blotting. The  $\beta$ -actin levels were measured as loading controls. The asterisks indicate statistically significant changes: \*\* $P \leq 0.01$  and \*\*\* $P \leq 0.001$ .

named this inducible FOXA1-expressing MDA-MB-231 Clone 2 as 231-FOXA1-ind cells, which demonstrated similar characteristics as those of the parent cells and 231-Con-ind cells (Figure S8), and we used  $2 \mu\text{g}/\text{mL}$  doxycycline for FOXA1 induction (FOXA1-On) in the subsequent experiments. The FOXA1-On caused a significant decrease in the cell numbers (Figure 2A) and stimulated the cell apoptosis, in which more positive TUNEL signals and apoptotic bodies were recorded (Figure 2B, 2C). The cell proliferation was also inhibited by FOXA1, as evidenced by the decreased numbers of EdU-positive cells in the FOXA1-On cells (Figure 2D). Further experiments revealed that FOXA1 inhibited the abilities of colony formation in the FOXA1-On cells (Figure 2E). In the FOXA1-On

cells, apoptosis-related caspase-3 was activated and the levels of proliferation-related PCNA [39] were dramatically decreased (Figure 2F).

*The repressive roles of FOXA1 in MDA-MB-231 cells were confirmed by transcriptomic analysis and in vivo tumor-grafted models*

To further investigate the repressive mechanisms of FOXA1 in MDA-MB-231 cells, we performed transcriptomic analysis between the samples of FOXA1-On and FOXA1-Off 231-FOXA1-ind cells (Table S1). The results of GO analysis revealed that a greater number of genes of apoptosis and lysosome pathways were activated while the genes of DNA replication, cell cycle, and ribosome pathways were inhibited after the induction of FOXA1 expres-

sion in the cells (**Figure 3A**). The genes related to apoptosis and cell cycle pathways were further enriched through GSEA analysis to confirm the activation of apoptosis and the inhibition of the cell cycle through FOXA1 in the cells (**Figure 3B**). Certain genes were selected as representative markers of apoptosis (such as BCL-2 interacting killer (BIK), which is the first member of the BH3-only pro-apoptotic proteins [7], and bound to the members of the Bcl-2 family to inhibit their anti-apoptotic functions [13]) and cell cycle (such as CDC25C [6] and MCM8 [31] that promoted cells cycle and DNA replication) for further testing and the changes in their expression were also marked out in a volcano plot (**Figure 3C**). The elevated levels of BIK and the decreased levels of CDC25C and MCM 8 were confirmed in the FOXA1-On cells (**Figure 3D, 3E**). To further analyze the repressive roles of FOXA1 to the cells *in vivo*, we implanted subcutaneous MDA-MB-231 cells or 231-FOXA1-ind cells at the left or right axilla, respectively, in the same BALB/c nude mouse. We noticed that FOXA1-Off 231-FOXA1-ind cells demonstrated a similar ability to form engrafted-tumors as that of the parent MDA-MB-231 cells in the animals (**Figure S9**). After the animals were fed with water supplemented with doxycycline to induce FOXA1-On in 231-FOXA1-ind cells, the growth of the FOXA1-On tumors was found to be significantly repressed (**Figure 3F**). Tumor samples were collected on day 27 of the experiment to reveal a significant decrease in the size and weight in the case of the FOXA1-On tumors (**Figure 3G**), whose tissue sections showed elevated signals of active caspase-3-cleaved subunits and FOXA1 (**Figure 3H**). Consequently, we observed that the levels of apoptosis-related BIK were increased while those of proliferation-related PCNA, CDC25C, and MCM8 were decreased in the FOXA1-On tumors (**Figure 3I, 3J**). These results demonstrated that the elevation of the FOXA1 levels repressed MDA-MB-231 cells by stimulating the expression of genes related to apoptosis and inhibiting the expression of genes related to cell proliferation.

### *ESR1 counteracted the repressive functions of FOXA1 in MDA-MB-231 cells*

Past studies reported that FOXA1 cooperated with ESR1 in regulating the gene expression in luminal breast cancer cells [9, 27] and that the

decreased expression of FOXA1 correlated with poor prognosis of basal breast cancers [23]. The TCGA clinical breast cancer samples (n=1122) revealed that the average level of ESR1 in the basal subgroup was lower than that in the normal breast tissues and the individual levels of ESR1 varied widely among the patients (**Figure S10**). To analyze whether the effects of FOXA1 on the survival of patients relied on the ESR1 levels, we built two ESR1-related subgroups of clinical samples, in which the ESR1<sup>High</sup> subgroup (n=349) or the ESR1<sup>Low</sup> subgroup (n=349) contained either the top 1/3 or the bottom 1/3 of the collected TCGA BRCA data, excluding the normal breast tissue samples (n=75). Our results revealed that patients with high levels of FOXA1 demonstrated a better performance in terms of survival compared to patients with low levels of FOXA1 in the ESR1<sup>Low</sup> subgroup (P=0.037), although the high levels of FOXA1 were noted to worsen the survival of patients in the ESR1<sup>High</sup> subgroup (P=0.002) (**Figure 4A**), suggesting that the FOXA1-improved survival in the patients relied on the poor expression status of ESR1 in their cancers. To evaluate whether ESR1 counteracted the repressive functions of FOXA1 observed above in MDA-MB-231 cells, we first analyzed the effects of the restored expression of ESR1 in 231-Con-ind cells and 231-FOXA1-ind cells, which possessed the same characteristics as the parent MDA-MB-231 cells. We generated ESR1-expressing 231-Con-ind cells (ESR1-231-Con-ind) or ESR1-expressing 231-FOXA1-ind cells (ESR1-231-FOXA1-ind) by infecting 231-Con-ind or 231-FOXA1-ind cells respectively, with the ESR1-expressing lentivirus. Both ESR1-231-Con-ind cells and ESR1-231-FOXA1-ind cells possessed similar characteristics, and showed a moderate decrease on cell viabilities compared to their control cells (**Figures S11 and S12**), consistent with the reported findings that the restoration of ESR1 expression in MDA-MB-231 cells inhibited the cell proliferation [12, 35, 43]. However, after FOXA1 was turned on in the ESR1-231-FOXA1-ind cells, no significant difference in the TUNEL signals was observed (**Figure 4B**), indicating that ESR1 abolished the FOXA1-mediated apoptosis in the cells. Interestingly, ESR1 and FOXA1 together enhanced the proliferation of the cells, as evidenced by the increased numbers of EdU-positive cells in the FOXA1-On groups of the cells (**Figure 4C**). The subsequent

## FOXA1 represses basal breast cancer cells

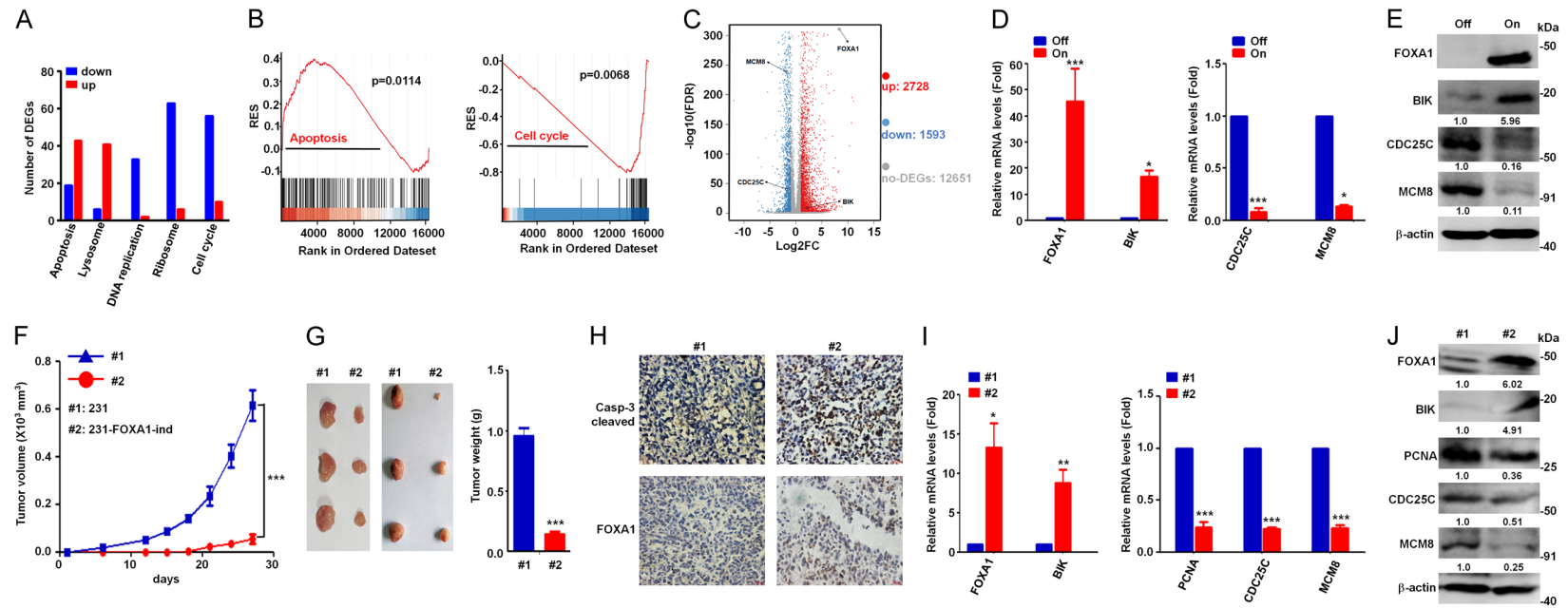


**Figure 3.** The repressive roles of FOXA1 in MDA-MB-231 cells were confirmed by transcriptomic analysis and *in vivo* tumor-grafted models. (A-C) The transcriptomic analysis of the induced expression of FOXA1 in 231-FOXA1-ind cells. Total RNAs of 231-FOXA1-ind cells treated with doxycycline (2  $\mu\text{g}/\text{mL}$ ) or without doxycycline (FOXA1-On or FOXA1-Off) were prepared at Day 2 post the treatment for RNA sequencing analysis. GO analysis showed the numbers of differentially expressed genes (DEGs, FDR <0.05,  $\log_2\text{FC} >1$ ) involved in signaling pathways such as apoptosis, DNA replication, cell cycle, ribosome, and lysosome pathways with R package “GEOquery” between the FOXA1-On and FOXA1-Off cells (A). The genes related to apoptosis and cell cycle pathways were further enriched by GSEA analysis to obtain the running enrichment score (RES) (B). The changes of mRNA levels of genes were plotted in a volcano plot (Red: up,  $\log_2\text{FC} \geq 1$ ; Blue: down,  $\log_2\text{FC} \leq -1$ ; Grey: not changed,  $-1 < \log_2\text{FC} < 1$ ). The dots representing selected genes (FOXA1, BIK, CDC25C, and MCM8) were marked out in the plot (C). (D, E) The changes of the mRNA and protein levels of FOXA1, BIK, CDC25C, and MCM 8 were confirmed by qPCR (D) and Western blotting (E) in the cell samples of the FOXA1-Off (Off) and FOXA1-On (On) cells. (F-H) The *in vivo* tumor-grafted models. BALB/c nude mice (n=6) were subcutaneously (S.C.) injected ( $5 \times 10^5$  cells/injection) with MDA-MB-231 cells at left axilla (group #1) and 231-FOXA1-ind cells at right axilla (group #2), and fed with water containing doxycycline (1 mg/mL) during the whole experimental period. The size of engrafted tumors was measured at the interval of three days and tumor samples were collected at Day 27 post the injection of the cells. The volumes of tumors were calculated by:  $V = \text{length} \times \text{diameter}^2 \times 1/2$ . Each data point represented the mean tumor volume in  $\text{mm}^3 \pm \text{SD}$  (F). Representative tumors harvested at Day 27 of the experimental period were imaged and the weight of the tumors were measured (G). The tumor tissue sections of the two groups were immunostained with FOXA1-specific or cleaved caspase-3-specific (Casp-3 cleaved) antibodies and typical pictures were taken by microscope (200 $\times$ ) (H). (I, J) Total RNAs and proteins were prepared with the harvested tumors and the pools of combined RNA and protein samples for the two groups were obtained. The mRNA and protein levels of FOXA1, BIK, PCNA, CDC25C, and MCM8 were examined by qPCR (I) and Western blotting (J). The asterisks indicate statistically significant changes: \* $P \leq 0.05$ , \*\* $P \leq 0.01$ , and \*\*\* $P \leq 0.001$ .

## FOXA1 represses basal breast cancer cells

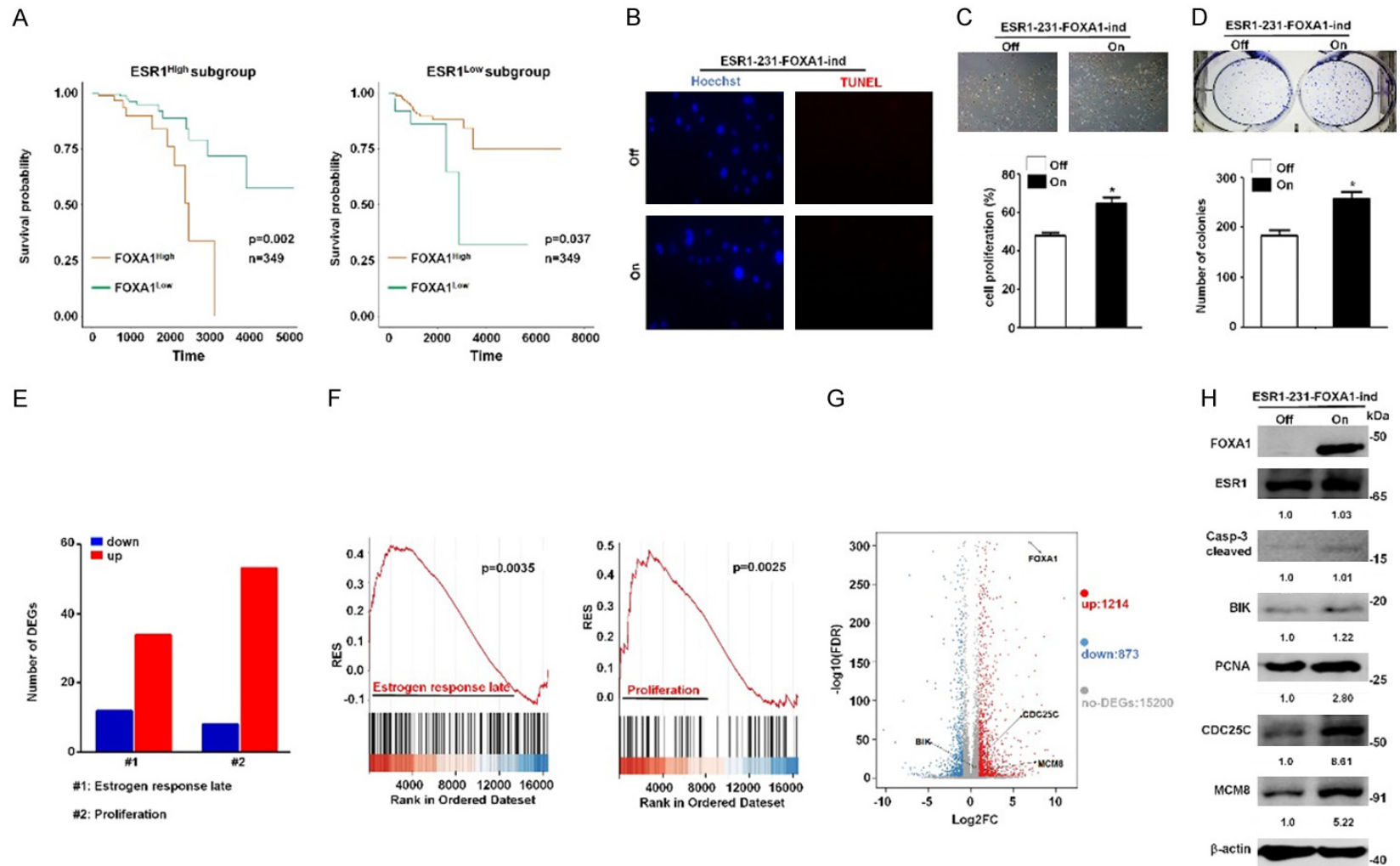


**Figure 4.** ESR1 counteracted the repressive functions of FOXA1 in MDA-MB-231 cells. (A) The FOXA1-improved survival in breast cancer patients relied on the low levels of ESR1 expression. The ESR1<sup>high</sup> subgroup (n=349) or the ESR1<sup>low</sup> subgroup (n=349) contained either the top 1/3 or the bottom 1/3 of the collected TCGA BRCA data set (n=1047) respectively according to the levels of ESR1 expression. FOXA1-related survival of patients in the ESR1<sup>high</sup> or ESR1<sup>low</sup> subgroup was fitted by the 'survfit' function and Kaplan-Meier curves were drawn by the 'ggsurv' function in the R package 'survival'. The cut-off value of FOXA1 high or low expression was determined by setting 'minprop' parameter to 0.1. (B) The elevated expression of FOXA1 did not stimulate apoptosis in ESR1-expressing MDA-MB-231 cells. ESR1-231-FOXA1-ind cells were treated with doxycycline (2  $\mu$ g/mL) (On) or not (Off) and the TUNEL assays were performed at Day 2 post the treatment. (C, D) The elevated expression of FOXA1 promoted proliferation in ESR1-expressing breast cancer cells. ESR1-231-FOXA1-ind cells were treated as above and the proliferation of the cells were measured at Day 2 post the treatment. The numbers of EdU-positive cells were counted to calculate the percentage of proliferative cells (C). The

## FOXA1 represses basal breast cancer cells

colony formation assays were performed and the cells ( $6 \times 10^2$  cells/well) were fixed at Day 14 post the treatment and the colonies were imaged by crystal violet staining. The numbers of colonies were counted and the graph represented the numbers  $\pm$  SD of colonies/well (D). (E-G) The transcriptomic analysis of ESR1-231-FOXA1-ind cells with the induction of FOXA1. Total RNAs of ESR1-231-FOXA1-ind cells treated with doxycycline (2  $\mu$ g/mL) or without doxycycline (FOXA1-On or FOXA1-Off) were prepared at Day 2 post the treatment for RNA sequencing analysis. GO analysis showed the numbers of differentially expressed genes (DEGs, FDR <0.05, log<sub>2</sub>FC >1) involved in signaling pathways such as Estrogen response late (#1) and Proliferation pathways (#2) with R package "GEOquery" between the FOXA1-On and FOXA1-Off cells (E). The genes related to Estrogen response late and Proliferation pathways were further enriched by GSEA analysis to obtain the running enrichment score (RES) (F). The changes of mRNA levels of genes were plotted in a volcano plot (Red: up, log<sub>2</sub>FC  $\geq$ 1; Blue: down, log<sub>2</sub>FC  $\leq$  -1; Grey: not changed, -1 < log<sub>2</sub>FC < 1). The dots representing selected genes (FOXA1, BIK, CDC25C, and MCM8) were marked out in the plot (G). (H) The changes of the levels of FOXA1, ESR1, Casp-3 cleaved, BIK, PCNA, CDC25C, and MCM 8 were confirmed by Western blotting in the cell samples of ESR1-231-FOXA1-ind cells under the FOXA1-Off (Off) and FOXA1-On (On) conditions. The asterisks indicate statistically significant changes: \*P $\leq$ 0.05 and \*\*P $\leq$ 0.01.

experiments demonstrated that ESR1 and FOXA1 together enhanced the abilities of colony formation in the cells (**Figure 4D**). Furthermore, we performed the transcriptomic analysis between the samples of FOXA1-On and FOXA1-Off of ESR1-231-FOXA1-ind cells (**Table S2**). The GO analysis revealed that more genes of late estrogen response and the proliferation pathways were activated in FOXA1-On ESR1-231-FOXA1-ind cells (**Figure 4E**). The GSEA analysis could enrich the genes related to late estrogen response and the proliferation pathways in the cells (**Figure 4F**). The changes in the levels of selected genes (i.e., FOXA1, BIK, CDC25C, and MCM8) were also marked out in a volcano plot (**Figure 4G**). In addition, the protein levels were measured for cells wherein no significant differences were detected for the levels of apoptosis-activated caspase-3 and BIK between FOXA1-Off and FOXA1-On conditions, albeit the levels of proliferation-related PCNA, CDC25C, and MCM-8 were increased dramatically in the FOXA1-On cells (**Figure 4H**). We further generated an inducible FOXA1-expressing MCF-7 cell line (7-FOXA1-ind) from MCF-7 cells expressing ESR1 and FOXA1 endogenously and noticed that FOXA1-On 7-FOXA1-ind cells demonstrated a proliferation-promoting phenotype similar as that of FOXA1-On ESR1-231-FOXA1-ind cells (**Figure S13**). Cumulatively, our results implicated that FOXA1 may play opposite roles in either promoting or repressing breast cancer cells depending on the levels of ESR1 in the cells.

### *ESR1 disrupted the transcriptional activities of FOXA1 on the BIK promoter in MDA-MB-231 cells*

In order to provide evidence that ESR1 obstructed the repressive functions of FOXA1 in MDA-

MB-231 cells, we investigated how ESR1 affected the transcriptional activities of FOXA1 on *BIK*. When the -1.8-kb promoter of *BIK* was scanned with the consensus FOXA1-DNA-binding sequence, we identified two putative FOXA1-binding sites at the regions -1206 bp to -1196 bp and -1786 bp to -1776 bp. Next, ChIP assays confirmed that FOXA1 bound to endogenous *BIK* promoter at regions around -1206 bp to -1196 bp, but not on the other tested regions in the FOXA1-On 231-FOXA1-ind cells (**Figure 5A**). Consistent with this finding, EMSA experiments showed that a FAM-labeled DNA probe, synthesized from the *BIK* promoter region from -1206 bp to -1196 bp, could form a DNA/protein complex with FOXA1 and that the addition of either an unlabeled probe (100 $\times$ ) or FOXA1-specific antibody disturbed the formation of the FOXA1/DNA complex, whereas the FAM-labeled mutated probe could not form the FOXA1/DNA complex (**Figure 5B**). These results together suggested that the *BIK* promoter could be activated directly by FOXA1 in the 231-FOXA1-ind cells. Furthermore, a correlation was noted between FOXA1 and *BIK* in the basal subgroup of the TCGA BRCA dataset (n=220, R=0.33, P<0.001) (**Figure 5C**), which indicated that FOXA1-mediated expression of *BIK* contributed to the better survival rate for patients in this subgroup with high levels of FOXA1 (**Figure 1B**). To determine whether ESR1 affected the FOXA1-stimulated expression of *BIK*, we performed additional ChIP assays with FOXA1-On ESR1-231-FOXA1-ind cell samples. We noted that the binding of FOXA1 to the endogenous *BIK* promoter was disrupted by the presence of ESR1 (**Figure 5D**). We further conducted EMSA experiments, wherein the nuclear extracts contained only the expressed FOXA1, the expressed ESR1, or the expressed FOXA1 and ESR1 combined. We noted that ESR1 alone

## FOXA1 represses basal breast cancer cells

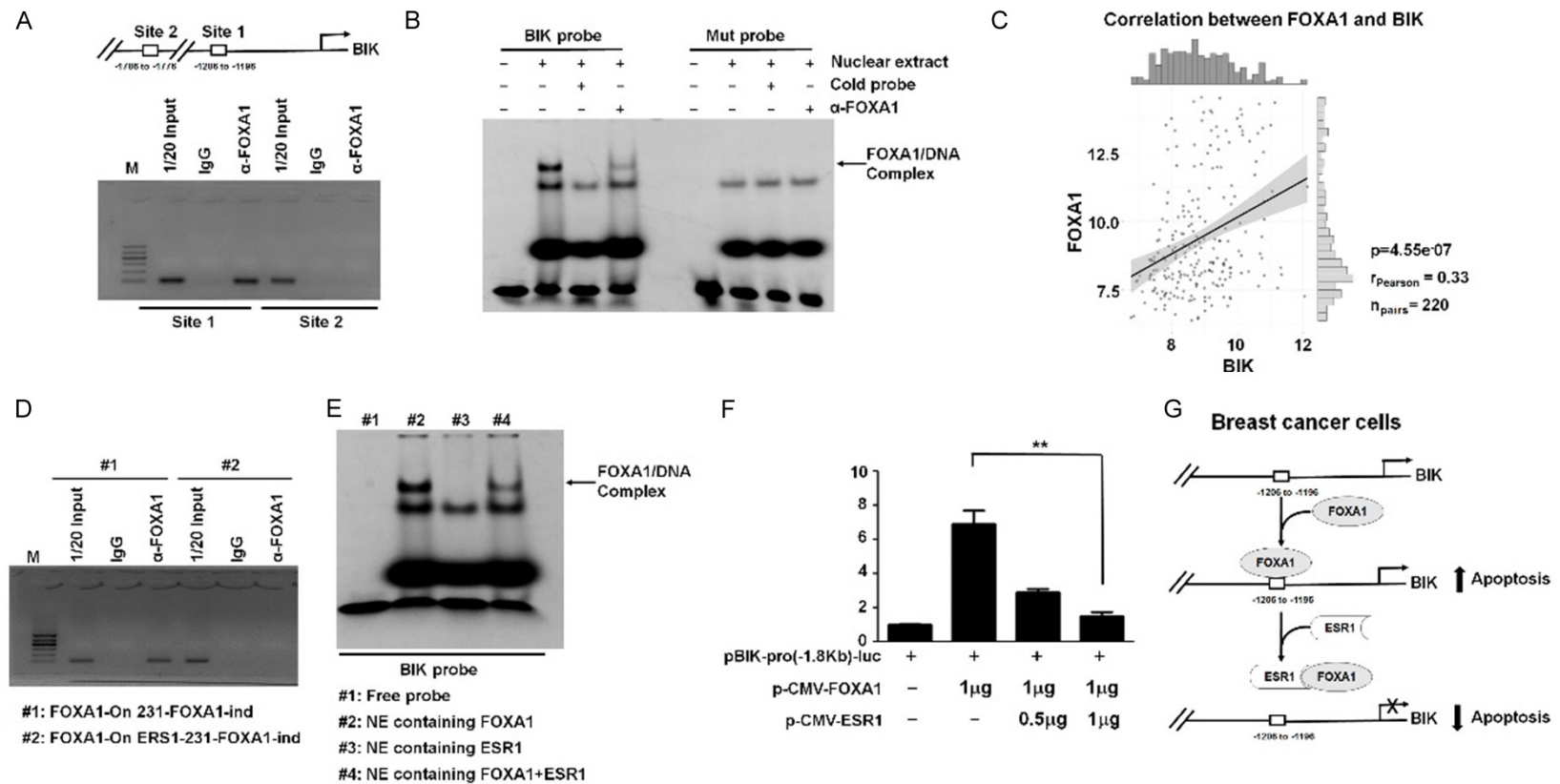


**Figure 5.** ESR1 disrupted the transcriptional activities of FOXA1 on the promoter of BIK gene in MDA-MB-231 cells. (A, B) FOXA1 bound to the endogenous BIK promoter region -1206 bp to -1196 bp. Gene sequence analysis was performed to predict two putative FOXA1 binding sites in -1.8 kb BIK promoter and two pairs of primers were designed for ChIP assays. The chromatin of FOXA1-On 231-FOXA1-ind cells was cross-linked, sonicated, and immunoprecipitated (IP) with either FOXA1 antibody or rabbit IgG. The amount of promoter DNA associated with the IP chromatin was measured by PCR with primers specific to BIK promoter regions -1206 bp to -1196 bp (Site 1) and -1786 bp to -1776 bp (Site 2) (A). Nuclear extracts were prepared from HEK293T cells transfected with pCMV-FOXA1 and used for EMSAs with a FAM-labeled DNA probe synthesized from Site 1 sequence. The unlabeled probe (100 $\times$ ) or 1  $\mu$ g of FOXA1 antibody ( $\alpha$ -FOXA1) was added to the reaction to show specificity of FOXA1. EMSAs with a FAM-labeled mutated probe were also performed (B). (C) The gene expression correlation analysis of FOXA1 and BIK in the TCGA basal breast cancer data set (n=220) was executed by using ggstatsplot package through R project. (D, E) ESR1 disrupted the binding of FOXA1 to Site 1 of BIK promoter. The chromatin samples of FOXA1-On 231-FOXA1-ind or FOXA1-On ESR1-231-FOXA1-ind cells were immunoprecipitated with either FOXA1 antibody or rabbit IgG. The amount of promoter DNA associated with the IP chromatin was measured by PCR with primers specific to BIK promoter Site 1 region (D). Nuclear extracts (NE) were prepared from HEK293T cells transfected with pCMV-FOXA1, pCMV-ESR1, or both, and used for EMSAs with a FAM-labeled DNA probe synthesized from Site 1 sequence (E). (F) The transcriptional activities of FOXA1 on the BIK promoter were abolished by ESR1. A luciferase reporter plasmid (1.5  $\mu$ g) containing the -1.8 kb BIK promoter and loading control pRL-CMV luciferase reporter plasmid (20 ng) were transfected into HEK293T cells with pCMV-FOXA1 (1  $\mu$ g) and different amount of pCMV-ESR1 (0, 0.5, 1  $\mu$ g). Protein lysates were prepared at Day 2 post transfection and used to measure dual luciferase enzyme activities. The asterisks indicate statistically significant changes: \*\* $P < 0.01$ . (G) The putative model of the disruption of the FOXA1 activities on the BIK promoter by ESR1. FOXA1 alone was able to stimulate apoptosis through activating the transcription of pro-apoptotic BIK in cells. ESR1 abolished the binding of FOXA1 on the BIK promoter and consequently inhibited the FOXA1-mediated apoptosis.

## FOXA1 represses basal breast cancer cells

could not bind to the DNA probe, rather it abolished the binding of FOXA1 to the probe (**Figure 5E**), implicating that ESR1 disrupted the activity of FOXA1 toward the stimulation of the BIK transcription in the cells. This speculation was further supported by the evidence that the increased expression of ESR1 significantly decreased the activation of FOXA1 on the BIK promoter (**Figure 5F**). We, therefore, proposed that FOXA1 could stimulate apoptosis at least by activating the transcription of *BIK*, while the expression of ESR1 could abolish the FOXA1-mediated apoptosis by preventing the binding of FOXA1 on the *BIK* promoter in the cells (**Figure 5G**).

### *ESR1 abolished the anti-tumor functions of FOXA1 in MDA-MB-231 cells in vivo*

To further establish the repressive roles of FOXA1 to MDA-MB-231 cells relying on the low levels of ESR1 *in vivo*, we subcutaneously implanted 231-FOXA1-ind cells or ESR1-231-FOXA1-ind cells at the left or right axilla, respectively, of the same BALB/c nude mouse. After feeding the animals with water containing doxycycline to induce the expression of FOXA1 in both the cells, the growth of ESR1-231-FOXA1-ind tumors was found to dramatically increase relative to those of 231-FOXA1-ind tumors (**Figure 6A**). The tumor samples collected on day 27 of the experiment showed a significant increase in size and weight of the ESR1-231-FOXA1-ind tumors (**Figure 6B**), whose tissue sections further exhibited decreased signals of cleaved caspase-3 and BIK (**Figure 6C**). We observed that ESR1 was highly expressed in the ESR1-231-FOXA1-ind tumors and that the levels of FOXA1 were similar between the two study groups (**Figure 6D, 6E**). Consequently, the levels of apoptosis-related BIK were decreased and the levels of proliferation-related PCNA, CDC25C, and MCM8 were increased in the samples of the ESR1-231-FOXA1-ind group (**Figure 6D, 6E**). The results together demonstrated that the expression of ESR1 abolished the repressive functions of FOXA1 in MDA-MB-231 cells *in vivo* by preventing the expression of pro-apoptosis genes and activating the expression of genes related to cell proliferation.

### Discussion

Our study results showed that FOXA1 alone stimulated apoptosis and inhibited the prolifer-

ation of FOXA1-low expressing basal breast cancer cells, thereby establishing an anti-tumor role of FOXA1 in this subgroup of breast cancer at the first time. The repressive functions of FOXA1 in this subgroup were further analyzed by transcriptomic analysis with the inducible FOXA1-expressing MDA-MB-231 cells. The 5 major pathways, including apoptosis, lysosome, DNA replication, cell cycle, and ribosome, were significantly affected by the FOXA1 expression, providing plausible mechanisms for FOXA1 to suppress the cells. The gene of the pro-apoptotic protein BIK that is bound directly to the members of the Bcl-2 family and stimulated apoptosis [7] was studied in detail as an example to confirm that FOXA1 could transcriptionally induce cell apoptosis. In addition, the levels of proliferation-related multiple Cyclins, Cdks, and MCMs were decreased by FOXA1, suggesting its anti-proliferative roles by repressing the levels of a broad range of cell cycle-promoting genes in the cells.

As a so-called “pioneering” transcription factor, FOXA1 functioned in the cell nuclei by regulating the transcription of its target genes. The protein of FOXA1 possessed a “winged helix” DNA-binding domain that mediated the binding of the monomer FOXA1 to the consensus DNA element A(A/T)T RTT (G/T)RY TY [37] on the promoters of its target genes, like that of the linker histones [14, 16]. The binding of FOXA1 to DNA could induce an open chromatin configuration, followed by the recruitment of other transcriptional regulators and chromatin remodeling [15, 41]. In most studies, FOXA1 was found to activate the transcription of its target genes; in conformance, our study demonstrated that FOXA1 directly bound to and activated the promoter of pro-apoptotic *BIK* and consequently induced cell apoptosis. Nonetheless, accumulated data suggest that a set of FOXA1 bindings to DNA also caused the transcriptional repression of its target genes [20, 32]. For example, we reported that FOXA1 repressed the transcription of genes such as *Nanog* [10] during the differentiation of pluripotent stem cells by recruiting Grg3 [40] to the promoter of *Nanog* and consequently inducing repressive histone modifications around this promoter [11]. Therefore, the abilities of FOXA1 to activate or inhibit the transcription of certain genes depended on specific situations of its protein-protein interactions in the cells, in which FOXA1 may take up markedly different biological roles.

## FOXA1 represses basal breast cancer cells

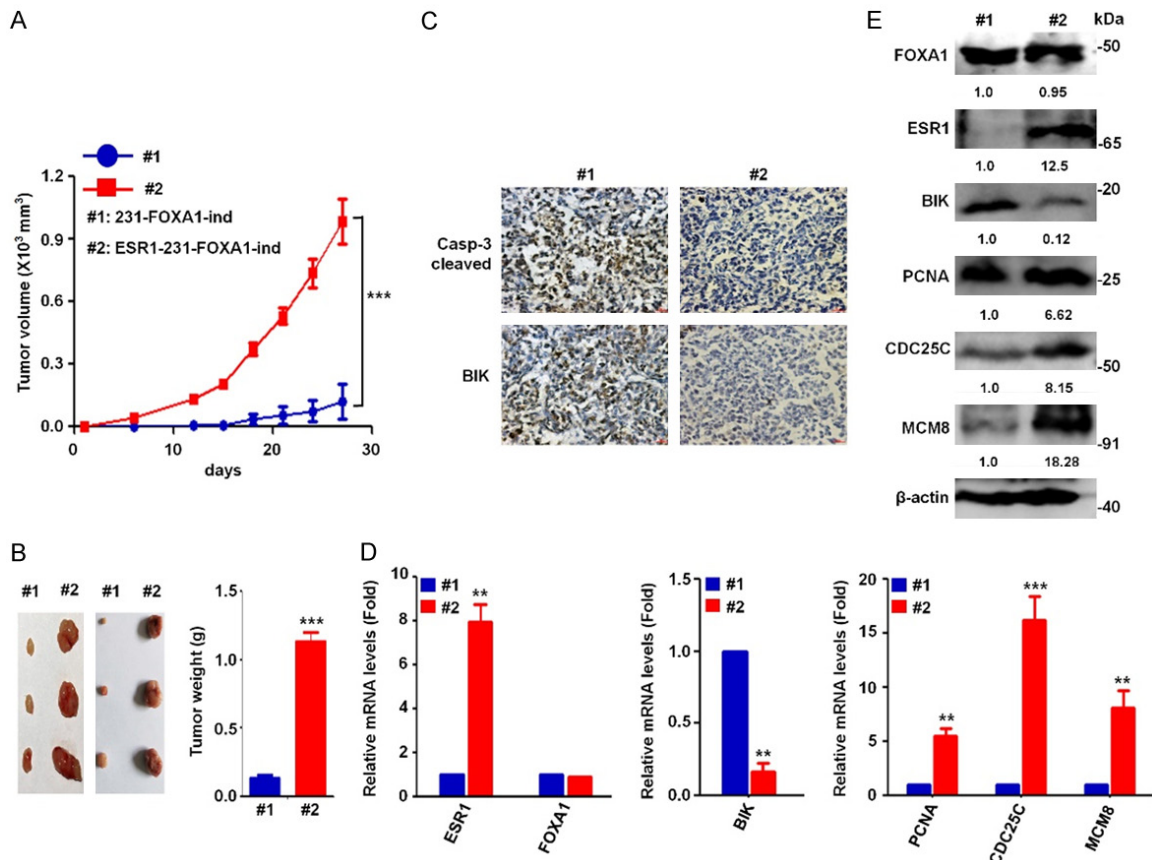


**Figure 6.** ESR1 abolished the anti-tumor functions of FOXA1 *in vivo*. BALB/c nude mice (n=6) were subcutaneously (S.C.) injected ( $5 \times 10^5$  cells/injection) with 231-FOXA1-ind cells at left axilla (group #1) and ESR1-231-FOXA1-ind cells at right axilla (group #2), and fed with water containing doxycycline (1 mg/mL) during the whole experimental period. (A) The size of engrafted tumors was measured at the interval of three days and tumor samples were collected at Day 27 post the injection of the cells. The volumes of tumors were calculated by:  $V = \text{length} \times \text{diameter}^2 \times 1/2$ . Each data point represented the mean tumor volume in  $\text{mm}^3 \pm \text{SD}$ . (B) Representative tumors harvested at Day 27 of the experimental period were imaged and the weight of the tumors were measured. (C) The tumor tissue sections of the two groups were immunostained with BIK-specific or cleaved caspase-3-specific (Casp-3 cleaved) antibodies and typical pictures were taken by microscope (200 $\times$ ). (D, E) Total RNAs and proteins were prepared with the harvested tumors and the pools of combined RNA and protein samples for the two groups were obtained. The mRNA and protein levels of FOXA1, ESR1, BIK, PCNA, CDC25C, and MCM8 were examined by qPCR (D) and Western blotting (E). The asterisks indicate statistically significant changes: \*\* $P \leq 0.01$ , and \*\*\* $P \leq 0.001$ .

The analysis of clinical samples revealed that the FOXA1-improved survival in breast cancer patients was correlated with the ESR1<sup>Low</sup> status and that high levels of FOXA1 in ESR1<sup>High</sup> breast cancers worsened the survival of patients (Figure 4A), implying that opposite roles (as either a tumor-suppressor or a tumor-stimulator) of FOXA1 depended on the levels of ESR1 in the breast cancer cells. Based on the molecular classification of breast cancer, a low level of ESR1 expression was generally detected in the basal breast cancer cells [49], which possessed niche cellular background to facilitate the apoptotic and anti-proliferative functions of FOXA1 independent of ESR1. On the

other hand, FOXA1 was found to promote the cell cycle progression [19] and/or inhibit apoptosis [52] of ER-positive luminal breast cancer cells, wherein FOXA1 occupied over half of the ESR1-binding sites in the genome and cooperated with ESR1 in regulating the gene expression [9], suggesting that ESR1 and FOXA1 together promoted the progression of ER-positive breast cancers. In this study, we detected ESR1 located in the nuclei (Figure S14) after its introduction into the FOXA1-expressing basal breast cancer MDA-MB-231 cells, although, consequently, FOXA1 lost its pro-apoptotic abilities and instead stimulated the cell proliferation. Accordingly, the transcrip-

tomic analysis provided further evidence suggesting that ESR1 and FOXA1 together activated the genes of the pathways of late estrogen response and the proliferation in these basal breast cancer cells (Figure 4F), suggesting significant differences relative to that when FOXA1 acted alone. In addition, considering the pro-apoptotic *B/K* promoter as an example, we demonstrated that FOXA1's binding and actions on this promoter was disrupted by the emergence of ESR1, which prevented FOXA1-mediated BIK induction and apoptosis in the cells. This observation provides a clue to explain how ESR1 counteracts the roles of FOXA1 as a tumor suppressor by altering the FOXA1 alone-regulated gene transcription. In the future, ChIP-seq analysis of the two proteins in the cells would help describe comprehensively and in detail the mechanisms behind FOXA1-led suppression of the cells independent of ESR1.

Based on the well-documented literature on the positive correlation between FOXA1 and ESR1, the pharmacological reduction of FOXA1 in patients with ESR1-positive luminal breast cancers would abrogate ESR1 signaling and possibly contribute to the efficacy of tamoxifen [22]. This postulate was disputed by a recent study indicating that the silencing of FOXA1 expanded a more aggressive and basal-like population of luminal breast cancer cells [3]. Supporting the role of FOXA1 in maintaining a less aggressive state of breast cancer, the overexpression of FOXA1 in basal breast cancer MDA-MB-231 cells induced E-cadherin expression and decreased the migratory capacity of the cells [30]; a similar phenotype was also recorded in our inducible FOXA1-expressing MDA-MB-231 cells (data not shown). Thus, while targeting FOXA1 in luminal breast cancer might be debatable, our present results confirmed that FOXA1 suppressed FOXA1-low expressing basal breast cancer, implicating its potential for use in developing therapeutic strategies for treating this subgroup of breast cancer.

### Acknowledgements

This work was supported by the National Natural Science Foundation of China (grant number 81773169 to Y.T., 81472718 to Y.T.), China Changsha Development and Reform Commission “Mass entrepreneurship and inno-

vation program” (2018-68) and “Innovation platform construction program” (2018-216).

### Disclosure of conflict of interest

None.

**Address correspondence to:** Drs. Li Yu and Yongjun Tan, College of Biology, Hunan University, Changsha 410082, Hunan, China. E-mail: yulihnbme@hnu.edu.cn (LY); yjtan@hnu.edu.cn (YJT)

### References

- [1] Alexandrou S, George SM, Ormandy CJ, Lim E, Oakes SR and Caldon CE. The proliferative and apoptotic landscape of basal-like breast cancer. *Int J Mol Sci* 2019; 20: 667.
- [2] Ang SL, Wierda A, Wong D, Stevens KA, Cascio S, Rossant J and Zaret KS. The formation and maintenance of the definitive endoderm lineage in the mouse: involvement of HNF3/forkhead proteins. *Development* 1993; 119: 1301-1315.
- [3] Bernardo GM, Bebek G, Ginther CL, Sizemore ST, Lozada KL, Miedler JD, Anderson LA, Godwin AK, Abdul-Karim FW, Slamon DJ and Keri RA. FOXA1 represses the molecular phenotype of basal breast cancer cells. *Oncogene* 2013; 32: 554-563.
- [4] Bernardo GM and Keri RA. FOXA1: a transcription factor with parallel functions in development and cancer. *Biosci Rep* 2012; 32: 113-130.
- [5] Besnard V, Wert SE, Hull WM and Whitsett JA. Immunohistochemical localization of Foxa1 and Foxa2 in mouse embryos and adult tissues. *Gene Expr Patterns* 2004; 5: 193-208.
- [6] Boutros R, Lobjois V and Ducommun B. CDC25 phosphatases in cancer cells: key players? Good targets? *Nat Rev Cancer* 2007; 7: 495-507.
- [7] Boyd JM, Gallo GJ, Elangovan B, Houghton AB, Malstrom S, Avery BJ, Ebb RG, Subramanian T, Chittenden T, Lutz RJ, et al. Bik, a novel death-inducing protein shares a distinct sequence motif with Bcl-2 family proteins and interacts with viral and cellular survival-promoting proteins. *Oncogene* 1995; 11: 1921-1928.
- [8] Bray F, Ferlay J, Soerjomataram I, Siegel RL, Torre LA and Jemal A. Global cancer statistics 2018: GLOBOCAN estimates of incidence and mortality worldwide for 36 cancers in 185 countries. *CA Cancer J Clin* 2018; 68: 394-424.
- [9] Carroll JS, Liu XS, Brodsky AS, Li W, Meyer CA, Szary AJ, Eeckhoutte J, Shao W, Hestermann EV, Geistlinger TR, Fox EA, Silver PA and Brown

## FOXA1 represses basal breast cancer cells

- M. Chromosome-wide mapping of estrogen receptor binding reveals long-range regulation requiring the forkhead protein FoxA1. *Cell* 2005; 122: 33-43.
- [10] Chambers I, Colby D, Robertson M, Nichols J, Lee S, Tweedie S and Smith A. Functional expression cloning of Nanog, a pluripotency sustaining factor in embryonic stem cells. *Cell* 2003; 113: 643-655.
- [11] Chen TH, He SJ, Zhang Z, Gao W, Yu L and Tan YJ. Foxa1 contributes to the repression of Nanog expression by recruiting Grg3 during the differentiation of pluripotent P19 embryonal carcinoma cells. *Exp Cell Res* 2014; 326: 326-335.
- [12] Chen XX, Ma NY, Zhou ZR, Wang ZL, Hu QC, Luo JR, Mei X, Yang ZZ, Zhang L, Wang XF, Feng Y, Yu XL, Ma JL and Guo XM. Estrogen receptor mediates the radiosensitivity of triple-negative breast cancer cells. *Med Sci Monit* 2017; 23: 2674-2683.
- [13] Chinnadurai G, Vijayalingam S and Rashmi R. BIK, the founding member of the BH3-only family proteins: mechanisms of cell death and role in cancer and pathogenic processes. *Oncogene* 2008; 27 Suppl 1: S20-29.
- [14] Cirillo LA, McPherson CE, Bossard P, Stevens K, Cherian S, Shim EY, Clark KL, Burley SK and Zaret KS. Binding of the winged-helix transcription factor HNF3 to a linker histone site on the nucleosome. *EMBO J* 1998; 17: 244-254.
- [15] Cirillo LA and Zaret KS. An early developmental transcription factor complex that is more stable on nucleosome core particles than on free DNA. *Mol Cell* 1999; 4: 961-969.
- [16] Clark KL, Halay ED, Lai E and Burley SK. Co-crystal structure of the HNF-3/fork head DNA-recognition motif resembles histone H5. *Nature* 1993; 364: 412-420.
- [17] Costa RH, Grayson DR and Darnell JE Jr. Multiple hepatocyte-enriched nuclear factors function in the regulation of transthyretin and alpha 1-antitrypsin genes. *Mol Cell Biol* 1989; 9: 1415-1425.
- [18] Coulouarn C, Factor VM, Andersen JB, Durkin ME and Thorgeirsson SS. Loss of miR-122 expression in liver cancer correlates with suppression of the hepatic phenotype and gain of metastatic properties. *Oncogene* 2009; 28: 3526-3536.
- [19] Eeckhoutte J, Carroll JS, Geistlinger TR, Torres-Arzayus MI and Brown M. A cell-type-specific transcriptional network required for estrogen regulation of cyclin D1 and cell cycle progression in breast cancer. *Genes Dev* 2006; 20: 2513-2526.
- [20] Eeckhoutte J, Lupien M, Meyer CA, Verzi MP, Shivdasani RA, Liu XS and Brown M. Cell-type selective chromatin remodeling defines the active subset of FOXA1-bound enhancers. *Genome Res* 2009; 19: 372-380.
- [21] Fernandes-Alnemri T, Litwack G and Alnemri ES. CPP32, a novel human apoptotic protein with homology to *Caenorhabditis elegans* cell death protein Ced-3 and mammalian interleukin-1 beta-converting enzyme. *J Biol Chem* 1994; 269: 30761-30764.
- [22] Fu XY, Huang C and Schiff R. More on FOX news: FOXA1 on the horizon of estrogen receptor function and endocrine response. *Breast Cancer Res* 2011; 13: 307.
- [23] Habashy HO, Powe DG, Rakha EA, Ball G, Paish C, Gee J, Nicholson RI and Ellis IO. Forkhead-box A1 (FOXA1) expression in breast cancer and its prognostic significance. *Eur J Cancer* 2008; 44: 1541-1551.
- [24] Hannenhalli S and Kaestner KH. The evolution of Fox genes and their role in development and disease. *Nat Rev Genet* 2009; 10: 233-240.
- [25] Haupt B, Ro JY and Schwartz MR. Basal-like breast carcinoma: a phenotypically distinct entity. *Arch Pathol Lab Med* 2010; 134: 130-133.
- [26] Holst F, Stahl PR, Ruiz C, Hellwinkel O, Jehan Z, Wendland M, Lebeau A, Terracciano L, Al-Kuraya K, Janicke F, Sauter G and Simon R. Estrogen receptor alpha (ESR1) gene amplification is frequent in breast cancer. *Nat Genet* 2007; 39: 655-660.
- [27] Hurtado A, Holmes KA, Ross-Innes CS, Schmidt D and Carroll JS. FOXA1 is a key determinant of estrogen receptor function and endocrine response. *Nat Genet* 2011; 43: 27-33.
- [28] Kaestner KH, Knochel W and Martinez DE. Unified nomenclature for the winged helix/forkhead transcription factors. *Genes Dev* 2000; 14: 142-146.
- [29] Lin L, Miller CT, Contreras JI, Prescott MS, Dagenais SL, Wu R, Yee J, Orringer MB, Misesk DE, Hanash SM, Glover TW and Beer DG. The hepatocyte nuclear factor 3 alpha gene, HNF3alpha (FOXA1), on chromosome band 14q13 is amplified and overexpressed in esophageal and lung adenocarcinomas. *Cancer Res* 2002; 62: 5273-5279.
- [30] Liu YN, Lee WW, Wang CY, Chao TH, Chen Y and Chen JH. Regulatory mechanisms controlling human E-cadherin gene expression. *Oncogene* 2005; 24: 8277-8290.
- [31] Maiorano D, Cuvier O, Danis E and Mechali M. MCM8 is an MCM2-7-related protein that functions as a DNA helicase during replication elongation and not initiation. *Cell* 2005; 120: 315-328.
- [32] Malik S, Jiang S, Garee JP, Verdin E, Lee AV, O'Malley BW, Zhang M, Belaguli NS and Oesterreich S. Histone deacetylase 7 and FoxA1 in estrogen-mediated repression of RPRM. *Mol Cell Biol* 2010; 30: 399-412.

## FOXA1 represses basal breast cancer cells

- [33] Mehta RJ, Jain RK, Leung S, Choo J, Nielsen T, Huntsman D, Nakshatri H and Badve S. FOXA1 is an independent prognostic marker for ER-positive breast cancer. *Breast Cancer Res Treat* 2012; 131: 881-890.
- [34] Myatt SS and Lam EW. The emerging roles of forkhead box (Fox) proteins in cancer. *Nat Rev Cancer* 2007; 7: 847-859.
- [35] Nott SL, Huang YF, Li XD, Fluharty BR, Qiu X, Welshons WV, Yeh S and Muyan M. Genomic responses from the estrogen-responsive element-dependent signaling pathway mediated by estrogen receptor alpha are required to elicit cellular alterations. *J Biol Chem* 2009; 284: 15277-15288.
- [36] Nucera C, Eeckhoutte J, Finn S, Carroll JS, Ligon AH, Priolo C, Fadda G, Toner M, Sheils O, Attard M, Pontecorvi A, Nose V, Loda M and Brown M. FOXA1 is a potential oncogene in anaplastic thyroid carcinoma. *Clin Cancer Res* 2009; 15: 3680-3689.
- [37] Overdier DG, Porcella A and Costa RH. The DNA-binding specificity of the hepatocyte nuclear factor 3/forkhead domain is influenced by amino-acid residues adjacent to the recognition helix. *Mol Cell Biol* 1994; 14: 2755-2766.
- [38] Perou CM, Sorlie T, Eisen MB, van de Rijn M, Jeffrey SS, Rees CA, Pollack JR, Ross DT, Johnsen H, Akslen LA, Fluge O, Pergamenschikov A, Williams C, Zhu SX, Lonning PE, Borresen-Dale AL, Brown PO and Botstein D. Molecular portraits of human breast tumours. *Nature* 2000; 406: 747-752.
- [39] Prelich G and Stillman B. Coordinated leading and lagging strand synthesis during SV40 DNA replication in vitro requires PCNA. *Cell* 1988; 53: 117-126.
- [40] Sekiya T and Zaret KS. Repression by Groucho/TLE/Grg proteins: genomic site recruitment generates compacted chromatin in vitro and impairs activator binding in vivo. *Mol Cell* 2007; 28: 291-303.
- [41] Serandour AA, Avner S, Percevault F, Demay F, Bizot M, Lucchetti-Miganeh C, Barloy-Hubler F, Brown M, Lupien M, Metivier R, Salbert G and Eeckhoutte J. Epigenetic switch involved in activation of pioneer factor FOXA1-dependent enhancers. *Genome Res* 2011; 21: 555-565.
- [42] Shang Y, Hu X, DiRenzo J, Lazar MA and Brown M. Cofactor dynamics and sufficiency in estrogen receptor-regulated transcription. *Cell* 2000; 103: 843-852.
- [43] Sinha S, Shukla S, Khan S, Tollefsbol TO and Meeran SM. Epigenetic reactivation of p21<sup>CIP1</sup>/WAF1 and KLOTHO by a combination of bioactive dietary supplements is partially ERalpha-dependent in ERalpha-negative human breast cancer cells. *Mol Cell Endocrinol* 2015; 406: 102-114.
- [44] Song L, Wei X, Zhang B, Luo XJ, Liu JW, Feng YS and Xiao XZ. Role of Foxa1 in regulation of bcl2 expression during oxidative-stress-induced apoptosis in A549 type II pneumocytes. *Cell Stress Chaperones* 2009; 14: 417-425.
- [45] Song Y, Washington MK and Crawford HC. Loss of FOXA1/2 is essential for the epithelial-to-mesenchymal transition in pancreatic cancer. *Cancer Res* 2010; 70: 2115-2125.
- [46] Sun YP, Tao CL, Huang XM, He H, Shi HQ, Zhang QY and Wu HH. Metformin induces apoptosis of human hepatocellular carcinoma HepG2 cells by activating an AMPK/p53/miR-23a/FOXA1 pathway. *Onco Targets Ther* 2016; 9: 2845-2853.
- [47] Tan YJ, Xie ZQ, Ding M, Wang ZD, Yu QQ, Meng L, Zhu H, Huang XQ, Yu L, Meng XX and Chen Y. Increased levels of FoxA1 transcription factor in pluripotent P19 embryonal carcinoma cells stimulate neural differentiation. *Stem Cells Dev* 2010; 19: 1365-1374.
- [48] Thorat MA, Marchio C, Morimiya A, Savage K, Nakshatri H, Reis-Filho JS and Badve S. Forkhead box A1 expression in breast cancer is associated with luminal subtype and good prognosis. *J Clin Pathol* 2008; 61: 327-332.
- [49] Valentin MD, da Silva SD, Privat M, Alaoui-Jamali M and Bignon YJ. Molecular insights on basal-like breast cancer. *Breast Cancer Res Treat* 2012; 134: 21-30.
- [50] Wang D, Garcia-Bassets I, Benner C, Li WB, Su X, Zhou YM, Qiu JS, Liu W, Kaikkonen MU, Ohgi KA, Glass CK, Rosenfeld MG and Fu XD. Reprogramming transcription by distinct classes of enhancers functionally defined by eRNA. *Nature* 2011; 474: 390-394.
- [51] Williamson EA, Wolf I, O'Kelly J, Bose S, Tanosaki S and Koeffler HP. BRCA1 and FOXA1 proteins coregulate the expression of the cell cycle-dependent kinase inhibitor p27(Kip1). *Oncogene* 2006; 25: 1391-1399.
- [52] Yamaguchi N, Ito E, Azuma S, Honma R, Yanagisawa Y, Nishikawa A, Kawamura M, Imai J, Tatsuta K, Inoue J, Semba K and Watanabe S. FoxA1 as a lineage-specific oncogene in luminal type breast cancer. *Biochem Biophys Res Commun* 2008; 365: 711-717.
- [53] Zhang Z, Yang C, Gao W, Chen TH, Qian TT, Hu J and Tan YJ. FOXA2 attenuates the epithelial to mesenchymal transition by regulating the transcription of E-cadherin and ZEB2 in human breast cancer. *Cancer Lett* 2015; 361: 240-250.

## FOXA1 represses basal breast cancer cells

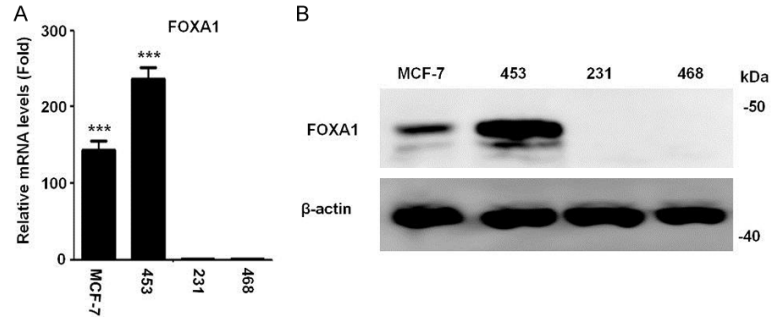


**Figure S1.** The levels of FOXA1 in different breast cancer cell lines. Non-basal breast cancer MCF-7 cells and basal breast cancer MDA-MB-453 (453), MDA-MB-231 (231), MDA-MB-468 (468), and MDA-MB-436 (436) cells were harvested to prepare total RNAs and protein lysates. (A) The mRNA levels of FOXA1 and GAPDH were measured by qPCR. The relative mRNA levels of FOXA1 were normalized to GAPDH and the mRNA levels of 231 cells were referred to as one. (B) The protein levels of FOXA1 were measured by Western blotting. The  $\beta$ -actin levels were measured as loading controls. The asterisks indicate statistically significant changes: \*\*\* $P \leq 0.001$ .

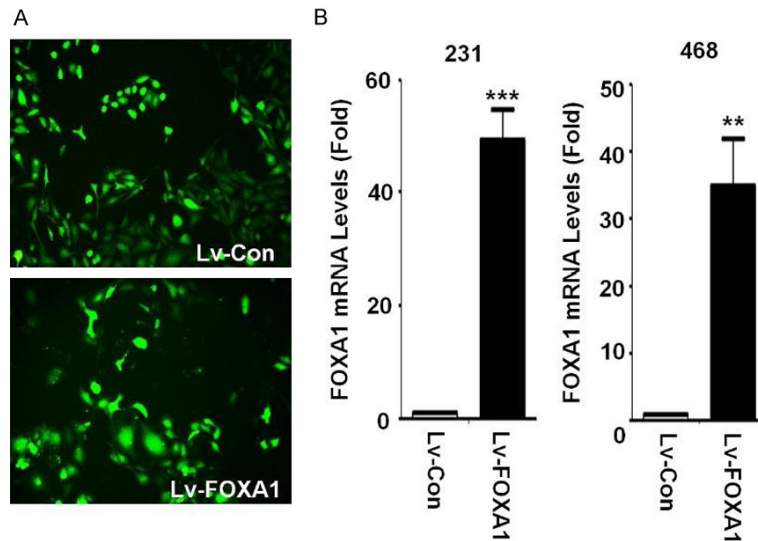


**Figure S2.** Lentivirus-mediated FOXA1 overexpression. MDA-MB-231 (231) and MDA-MB-468 (468) cells were infected by FOXA1-expressed lentivirus (Lv-FOXA1) or control lentivirus (Lv-Con) (20 pfu/cell). (A) The fluorescent signals of GFP were detected by fluorescent microscopy 2 days after infection. (B) Total RNAs were prepared from the cell samples 2 days after infection. The mRNA levels of FOXA1 and GAPDH were measured by qPCR and relative mRNA levels were normalized to GAPDH. The asterisks indicate statistically significant changes: \*\*\* $P \leq 0.001$ .

## FOXA1 represses basal breast cancer cells

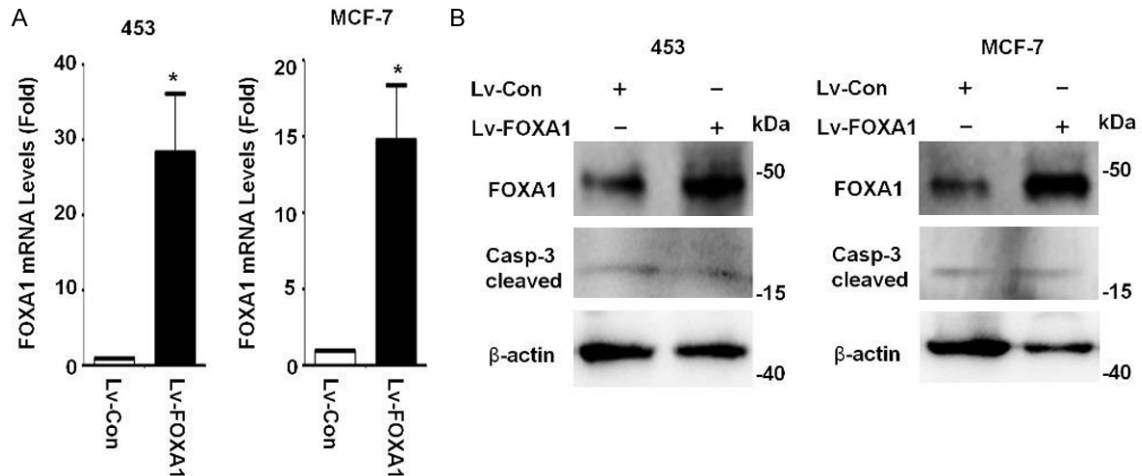


**Figure S3.** Elevated expression of FOXA1 did not affect the levels of apoptosis in MDA-MB-453 and MCF-7 cells. MDA-MB-453 and MCF-7 cells were infected by FOXA1-expressed lentivirus (Lv-FOXA1) or control lentivirus (Lv-Con) (20 pfu/cell). (A) Total RNAs were prepared from the cell samples 2 days after infection. The mRNA levels of FOXA1 and GAPDH were measured by qPCR and relative mRNA levels were normalized to GAPDH. The asterisks indicate statistically significant changes: \* $P \leq 0.05$ . (B) The protein levels of FOXA1 and activated caspase-3 (Casp-3 cleaved) were measured by Western blotting. The  $\beta$ -actin levels were measured as loading controls.

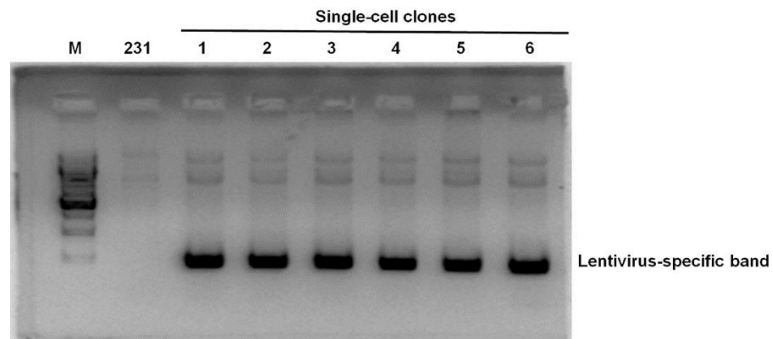


**Figure S4.** The selection of inducible FOXA1-expressing MDA-MB-231 cell lines. MDA-MB-231 (231) cells were infected with the FOXA1-inducible expression lentivirus (20 pfu/cell, 48 hrs) and treated with puromycin (2  $\mu\text{g}/\text{mL}$ , 72 hrs) for cell line selection. The genomic DNA samples extracted from 231 cells or the cells of selected single-cell clones (1-6) were used for PCR with a pair of primers specific for the puromycin-resistant gene in the lentivirus vector. The products of PCR were separated and visualized by agarose gel.

## FOXA1 represses basal breast cancer cells

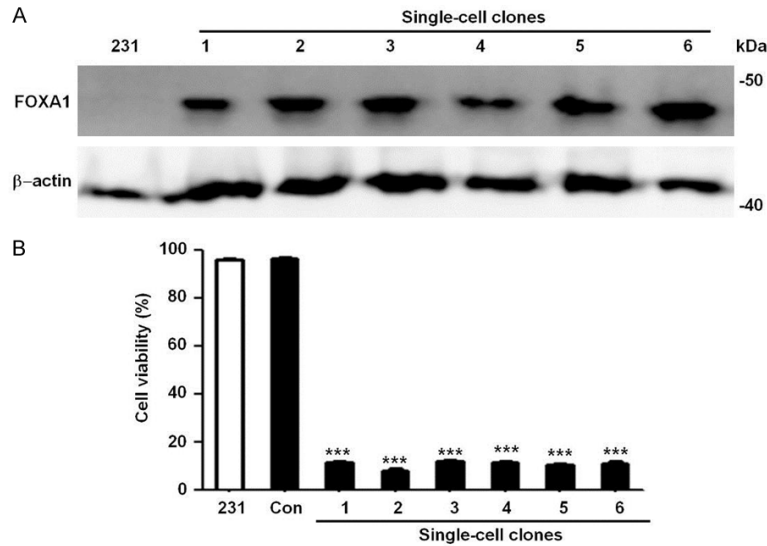


**Figure S5.** The expression of FOXA1 was induced by doxycycline in the selected clones of inducible FOXA1-expressing MDA-MB-231 cells. (A) The cells of the selected clones (1-6) of inducible FOXA1-expressing MDA-MB-231 cells were treated with doxycycline (2  $\mu$ g/mL) and were harvested to prepare protein lysates 2 days after the treatment. The protein levels of FOXA1 and  $\beta$ -actin were measured by Western blotting. (B) The cells of the selected clones (1-6) mentioned above were treated with doxycycline (2  $\mu$ g/mL) and the cell viability was measured 2 days after the treatment. MDA-MB-231 cells (231) and 231-Con-ind cells (Con) were used as the control. The asterisks indicate statistically significant changes: \*\*\* $P \leq 0.001$ .

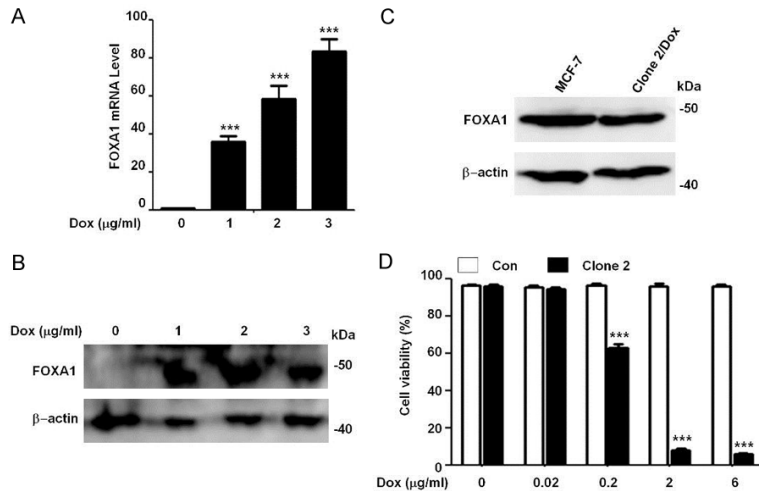


**Figure S6.** The dose determination of doxycycline for the induction of FOXA1. The cells of Clone 2 from [Figure S4](#) were chosen, treated with different dosages of doxycycline (1, 2, and 3  $\mu$ g/mL), and harvested to prepare total RNA and proteins 2 days after the treatment. The levels of FOXA1 were examined by qPCR (A) and Western blotting (B). (C) The comparison of FOXA1 levels in MCF-7 cells and doxycycline-treated Clone 2 cells. The protein lysates of MCF-7 cells and Clone 2 cells treated with doxycycline (2  $\mu$ g/mL, 48 hrs) were prepared for Western blotting to measure the protein levels of FOXA1 and  $\beta$ -actin. (D) The cells of Clone 2 were treated with different dosages of doxycycline (0, 0.02, 0.2, 2 and 6  $\mu$ g/mL) and the cell viability was measured 2 days after the treatment. 231-Con-ind cells (Con) were used as the control. The asterisks indicate statistically significant changes: \*\*\* $P \leq 0.001$ .

## FOXA1 represses basal breast cancer cells

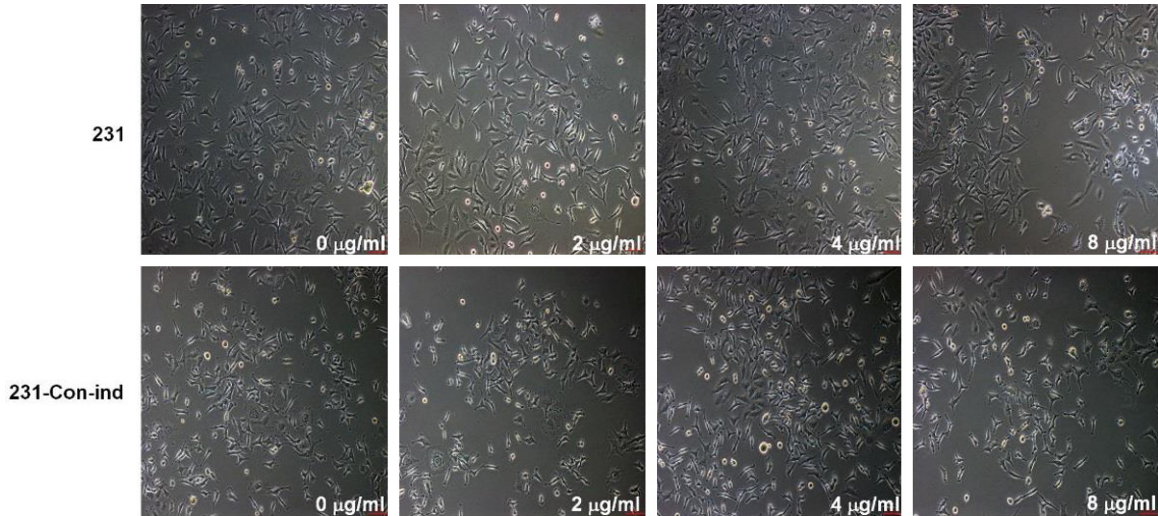


**Figure S7.** No obvious toxic effects were observed in the cells post the doxycycline treatment. MDA-MB-231 cells and 231-Con-ind cells were treated with different dosages of doxycycline (2, 4, 8 µg/mL) and the images were taken 2 days after the treatment.

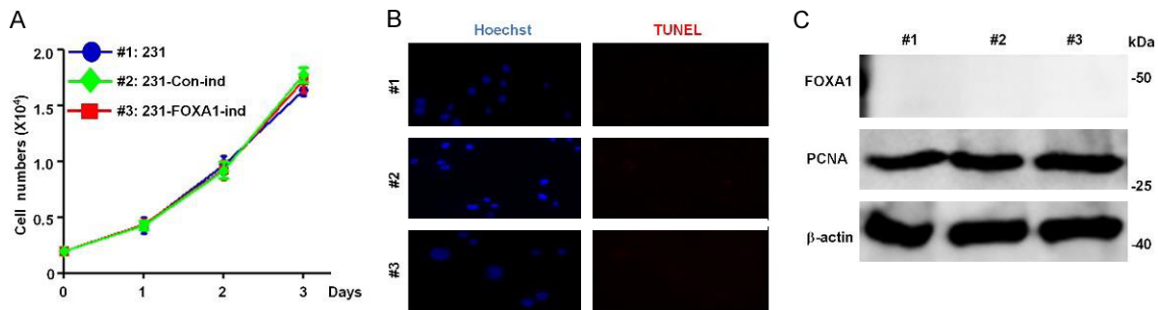


**Figure S8.** The comparison of MDA-MB-231 cells, 231-Con-ind and 231-FOXA1-ind cells. (A) No difference in the cell growth curve between MDA-MB-231 cells (#1), 231-Con-ind cells (#2) and 231-FOXA1-ind cells (#3). (B) No difference in apoptosis between the three cell lines. TUNEL assays were performed. (C) The protein lysates were prepared from the three cell lines and the levels of FOXA1 and PCNA were examined by Western blotting. The β-actin levels were measured as loading controls.

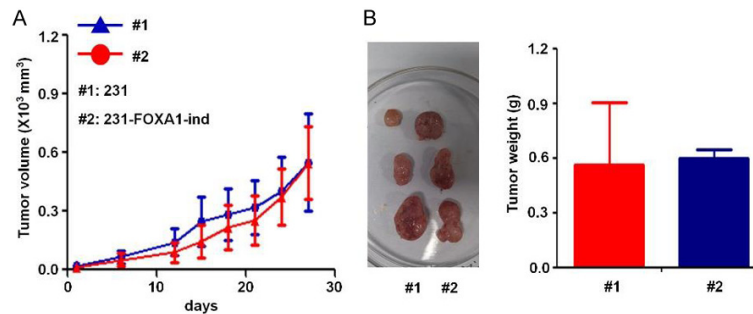


**Figure S9.** The ability of MDA-MB-231 and 231-FOXA1-ind cells to form transplanted tumors was similar. (A) BALB/c nude mice (n=3) were subcutaneously injected ( $5 \times 10^5$  cells/injection) with MDA-MB-231 cells at the left axilla (#1) and 231-FOXA1-ind cells at the right axilla (#2). The size of transplanted tumors was measured at three-day intervals. Each data point represents the mean tumor volume in mm<sup>3</sup> ± SD. (B) The tumors harvested on day 36 of the experimental period were imaged and the tumor weight was measured.

## FOXA1 represses basal breast cancer cells

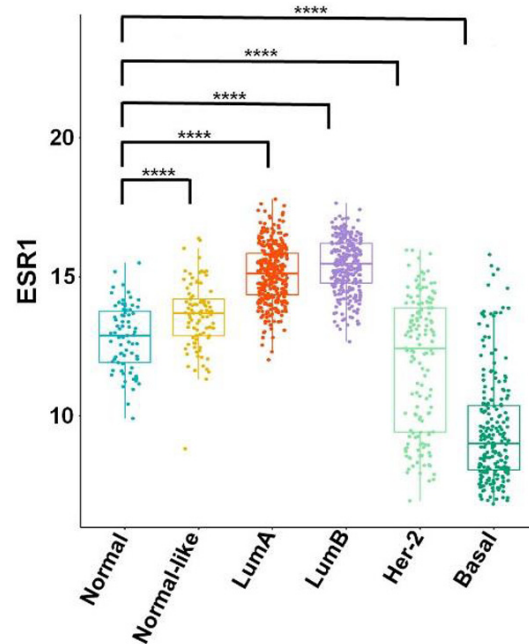


**Figure S10.** The levels of ESR1 in normal breast tissue and the five subtypes (Normal, n=75; Normal-like, n=89; LumA, n=318; LumB, n=275; Her-2, n=145; and Basal, n=220) of breast cancer from the clinical breast cancer samples (the TCGA BRCA data set, n=1122).

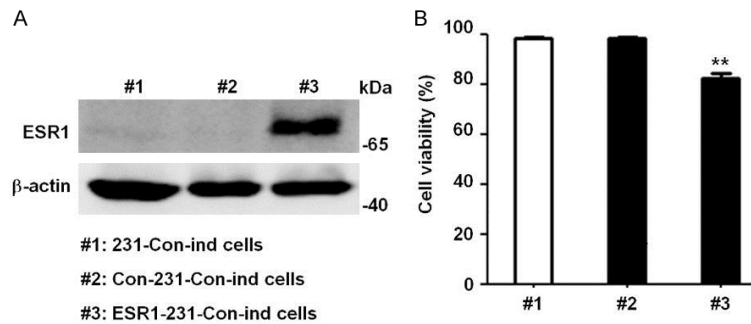


**Figure S11.** The elevated levels of ESR1 in basal breast cancer cells decreased cell viability. (A) 231-Con-ind cells (#1) were infected with Lv-Con (20 pfu/cell) to obtain Con-231-Con-ind cells (#2) or with ESR1-expressed lentivirus (20 pfu/cell) to obtain ESR1-231-Con-ind cells (#3). Cells were harvested to prepare protein lysates and protein levels of ESR1 and  $\beta$ -actin were measured by Western blotting. (B) Cells from cell lines #1, #2, and #3 (2,000 cells/well) were cultured and cell viability was measured after 48 hours.

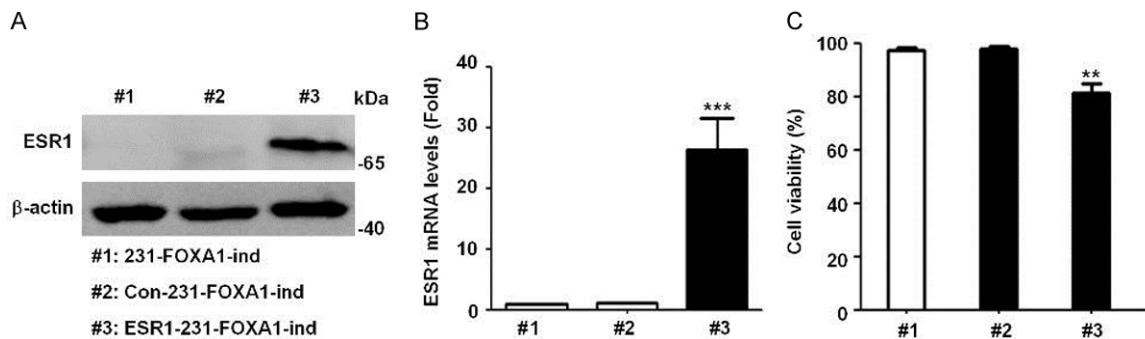


**Figure S12.** The construction of ESR1-expressing 231-FOXA1-ind cells. (A) 231-FOXA1-ind cells were infected with Lv-Con (20 pfu/cell) to obtain Con-231-FOXA1-ind cells or with ESR1-expressed lentivirus (20 pfu/cell) to obtain

## FOXA1 represses basal breast cancer cells

ESR1-231-FOXA1-ind cells. Protein levels of ESR1 and  $\beta$ -actin were measured by Western blotting. (B) 231-FOXA1-ind cells (#1), Con-231-FOXA1-ind cells (#2), and ESR1-231-FOXA1-ind cells (#3) were harvested to prepare total RNAs. The mRNA levels of ESR1 were measured by qPCR. Relative mRNA levels were normalized to GAPDH and the levels of 231-FOXA1-ind cells were referred to as one. (C) Cells from cell lines #1, #2, and #3 (2,000 cells/well) were cultured and cell viability was measured after 48 hours.

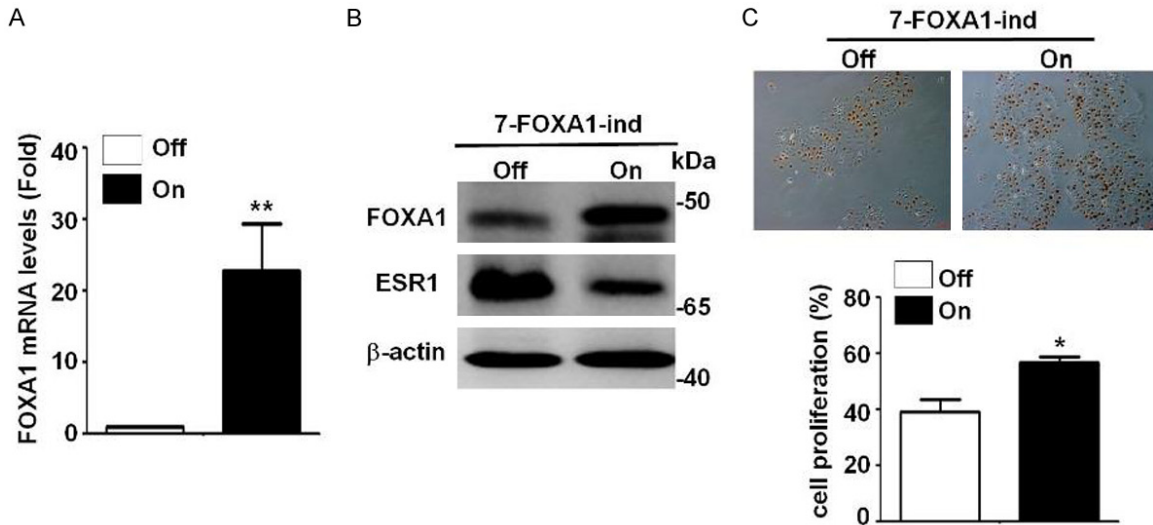


**Figure S13.** The consequence of the FOXA1 overexpression in ESR1-positive MCF-7 cells. MCF-7 cells were infected with the FOXA1-inducible expression lentivirus (20 pfu/cell, 48 hrs) and treated with puromycin (2  $\mu$ g/ml, 72 hrs) to generate 7-FOXA1-ind cells. (A, B) 7-FOXA1-ind cells were treated with doxycycline (2  $\mu$ g/ml) (On) or without the treatment (Off) and the mRNA levels of FOXA1 were examined by qPCR (A) and the protein levels of FOXA1 and ESR1 were detected by Western blotting (B). (C) The elevated expression of FOXA1 promoted proliferation in 7-FOXA1-ind cells. The FOXA1-Off (Off) and FOXA1-On (On) cells were stained with EdU and the numbers of EdU-positive cells were counted to calculate the percentage of proliferative cells. The asterisks indicate statistically significant changes: \* $P \leq 0.05$  and \*\* $P \leq 0.01$ .

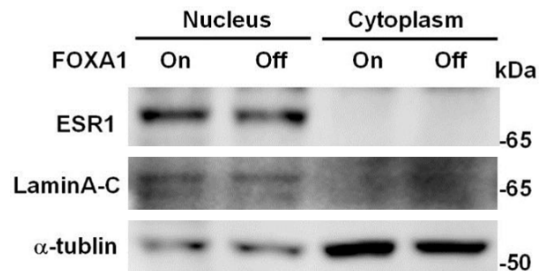


**Figure S14.** Nuclear localization of ESR1 in ESR1-231-FOXA1-ind cells. The ESR1-231-FOXA1-ind cells from FOXA1-off and FOXA1-On conditions were harvested to prepare cytoplasmic and nuclear proteins. The levels of ESR1 in the cytoplasm and the nucleus were examined by Western blotting.  $\alpha$ -Tubulin or LaminA/C was used as a cytoplasmic or nuclear marker respectively.